Geomorphology 480 (2025) 109750

Contents lists available at ScienceDirect

Geomorphology

journal homepage: www.journals.elsevier.com/geomorphology

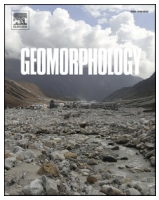

Deciphering sediment connectivity dynamic in traditional water-meadows (*lameiros*)

T. Bertocco [a,b,c], T. de Figueiredo [a,b], A. Paz-González [c], A. García-Tomillo [c], M. López-Vicente [c,d,*]

[a] Centro de Investigação de Montanha (CIMO), Instituto Politécnico de Bragança, Campus de Santa Apolónia, 5300-253 Bragança, Portugal
[b] Laboratório Associado para a Sustentabilidade e Tecnologia em Regiões de Montanha (SusTEC), Instituto Politécnico de Bragança, Campus de Santa Apolónia, 5300-253 Bragança, Portugal
[c] Group Aquaterra, Interdisciplinary Centre of Chemistry and Biology, CICA-UDC, Universidade da Coruña, 15071 A Coruña, Spain
[d] GEOFOREST, Departamento de Ciencias Agrarias y del Medio Natural, Escuela Politécnica Superior de Huesca, Instituto de Investigación en Ciencias Ambientales (IUCA), Universidad de Zaragoza, Ctra. Cuarte s/n, 22071 Huesca, Spain

ARTICLE INFO

Keywords:
Structural connectivity
Functional connectivity
Sediment source area
Sedimentation-prone area

ABSTRACT

Lameiros are traditional man-made water-meadows located at the bottom of the valleys in northern Portugal and northwestern Spain. Although *lameiros* act as hydrological and sediment accumulation regulators, this process has never been quantified in a spatially distributed manner (maps), nor have its temporal variations. For the first time, the role of *lameiros* in sediment connectivity is calculated by using the aggregated index of sediment connectivity (AIC) in two medium-size ungauged headwater basins with permanent and seasonal streams. Index parameterization was done in detail, including field surveys to distinguish the type, in-use ($n = 21$) or abandoned ($n = 78$), of *lameiros* and their water availability, well ($n = 89$) or poor ($n = 10$) irrigated. Different sedimentological scenarios that occur throughout the year were computed considering the net soil loss at the basin scale (target: watercourses; common conditions with the whole basin activated) and temporary accumulation in watercourses (target: outlet; dry conditions with sediment transport limited to the streams). The three erosive periods that happen during the year, i.e. high, medium and low rainfall erosivity, were simulated with long, average and short watercourses. Results of structural connectivity proved that the role played by each input (land-use, soil permeability, rainfall erosivity, slope gradient, drainage area, roughness of the terrain) on sediment connectivity strongly depended on the spatial location of each landscape unit regarding the selected target and not only on their own values. This fact explained the lower connectivity obtained in the abandoned *lameiros* than that found in the in-use *lameiros*. Map analysis indicated that during the dry period from May to September overland flow was restricted to the streams, sediment supply from slopes to *lameiros* was limited and the temporarily accumulated sediment in *lameiros* may be remobilized, while during the wet (January–April) and rainy (October–December) periods sediment supply from active slopes to *lameiros* was high and sediment delivery from *lameiros* to stream was relatively lower, acting as sedimentation-prone areas. Indeed, poor-irrigated *lameiros* had greater connectivity than well-irrigated *lameiros*. Connectivity of *lameiros* with their contributing areas (target: *lameiros*) was higher than that of the remaining land uses with the outlet and watercourses, proving the high sediment accessibility of this landscape feature. Index output performed well against available data of soil depth measured both in the *lameiros* and slopes. Multi-target computation of structural and functional connectivity concluded that sedimentation in *lameiros* prevailed against sediment delivery, although both processes occurred simultaneously throughout the year. This study suggests the convenience of preserving *lameiros* with some form of legal protection.

* Corresponding author at: Group Aquaterra, Interdisciplinary Centre of Chemistry and Biology, CICA-UDC, Universidade da Coruña, 15071 A Coruña, Spain.
E-mail addresses: manuel.lopez.vicente@udc.es, manuel.lopezv@unizar.es (M. López-Vicente).

https://doi.org/10.1016/j.geomorph.2025.109750
Received 17 April 2024; Received in revised form 21 March 2025; Accepted 2 April 2025
Available online 7 April 2025

1. Introduction

Soil detachment by water erosion and sediment transport are directly related to land use and management, and if associated with mountainous regions, energy relief intensifies soil erosion, and consequently sediment redistribution (Bakker et al., 2008). In mountainous areas, among land uses, agriculture, urbanization, and bare land present a high potential contribution to altering the balance between soil loss and deposition, and thus on sediment dynamics (Barreiro-Lostres et al., 2015; Xu et al., 2023), resulting in high sedimentation rates (Tang et al., 2020; Mangi et al., 2022). Forests, scrublands, and pasture, on the other hand, have a lower potential for sediment transport (Nadal-Romero et al., 2013; Tola and Shetty, 2021); but forest fires (Vieira et al., 2018) and forest road construction (Doten et al., 2006) bring a direct impact on sediment production and transport. In upland basins, vegetation can also trigger sediment yield reduction (Fortesa et al., 2020). However, pastures, in particular, when poorly managed can accelerate the processes of surface runoff and soil erosion, resulting in extensive land degradation (Kasai et al., 2005; Stavi et al., 2020). Despite the studies based on sediment delivery in mountain areas, the role and direct contribution of pastures in sediment connectivity, specifically water-meadows, at the basin scale have not yet been explored.

In the mountainous areas located in northern Portugal and northwestern Spain (mainly in Galicia and Asturias autonomous communities, and the provinces of León and Zamora), the presence of traditional water-meadows (called *lameiros* in Portuguese and Galician) is of great relevance for having unique characteristics with high landscape value (Pires et al., 1994). *Lameiros* are permanent pastures with resident vegetation (e.g., *Arrhenatherum elatius*, *Holcus lanatus*, *Plantago lanceolata*, *Dactylis glomerata*, *Anthoxanthum odoratum*, etc.; Poças et al., 2009) subject to soil and climate conditions (Poças et al., 2006) and can be classified according to water availability (irrigated, imperfectly irrigated, and rainfed *lameiros*), utilization regime (pasture, grass, and hay *lameiros*), and location (sloping hillside, mid-slope and valley *lameiros*) (Teles, 1970; Pires et al., 1994; van den Dries, 2002). The origin of the name *lameiros* comes from the muddy appearance of the pastures after saturation by water or flooding. They appear near the water lines, and thus, they have a great availability of water, besides having a fine texture and contain a high content of organic matter in composition (Vieira et al., 2000; Pereira et al., 2003). During the seventh to tenth centuries, along with the occurrence of new settlements in mountain areas, these marshes were created by human action, from the deforestation of humid forests presented there, to serve as pastures. In North and Center Portugal, *lameiros* were widespread and productive from the fourteenth century on (Pereira and Sousa, 2005; Ribeiro and Monteiro, 2014). According to Poças et al. (2007), *lameiros* create a discontinuity in the landscape and play an extremely relevant role, since their ecosystem contributes to the landscape, environment, and tourist, cultural and economic services. On the ecological side, they have great diversity in fauna and flora species, are essential in the spatial dynamics of nutrients and sediments, and contribute to the hydrological regulation and soil formation and consolidation. Besides, they may act as barriers against forest fire propagation. In terms of economic functionality, they are very productive and generate a source of food for animals and, consequently, income for local farmers (Aguiar et al., 2019). In the literature, there are studies on the effects of *lameiros* management from botanical and ecological (Poças et al., 2012, 2013; Fogaça-Neto, 2022), and hydrological (Bertocco, 2021; Ranzan, 2020) outlooks. Despite all these benefits, no published study addresses the role of *lameiros* in sediment transport processes at the basin scale. Besides, no study has identified the months or periods in which the accumulation of sediment occurs in the *lameiros*. This study sheds light on this topic and for the first time, sediment connectivity is calculated in headwater basins with presence of *lameiros*.

An important attribute in the study of basins is sediment connectivity (SC), which is characterized by the transfer of soil particles and sediments through the water along the landscape, i.e., it is the degree to which sediments are connected across a watershed or hydrological unit (Cavalli et al., 2013; López-Vicente et al., 2020). More specifically, SC includes two concepts: structural connectivity that is the potential of sediment movement considering the properties of a system on an average temporal scenario (e.g. during summer, winter, average annual, rainy/dry season, etc.); and functional connectivity that refers to the actual transfer of water and sediment through the system over the course of a specific event, episode or date (e.g. Dorothea storm; December 10th 2010) (López-Vicente and Ben-Salem, 2019; González-Romero et al., 2021; Wu et al., 2023). Recently, a refinement of these concepts were done by Najafi et al. (2021) who link functional and structural sediment connectivities to sediment availability and accessibility, respectively. Therefore, functional sediment connectivity refers the volume of sediment available for transport, while structural sediment connectivity shows the possibility of available sediments to be transported, and their pathways. Low functional sediment connectivity will lead to inefficiency of sediment delivery despite a high structural sediment connectivity and vice versa. Almost two decades ago, Borselli et al. (2008) developed the index of runoff and sediment connectivity (IC), based on GIS tools, which was later adapted by Cavalli et al. (2013) for mountainous areas with low vegetation cover. IC is a flexible approach that can be adapted to the specific conditions of any site in terms of evaluating the impedance of sediment transport with distinct metrics, such as the stream power index in Himalayan basins (Swarnkar et al., 2020) or Manning's coefficient in Brazil (Zanandrea et al., 2021). More recently, López-Vicente and Ben-Salem (2019) proposed the aggregated index of connectivity (AIC) that estimated structural and functional connectivity, by means of incorporating the rainfall erosivity, roughness of the terrain, and soil permeability factors. Both IC and AIC are suitable and widely applied in recent studies in the investigation of sediment connectivity in Mediterranean areas such as slopes (González-Romero et al., 2022), basins, and sub-basins (López-Vicente et al., 2021; van der Grift, 2021), even at the large basin and regional scale for the analysis of sediment connectivity in monthly and annual time (Wu et al., 2023).

This study evaluates the role of *lameiros* in the spatial pattern and temporal dynamic of sediment connectivity as dis-connectivity landscape features. To achieve this goal, AIC is used to generate the maps of structural and functional (seasonal) SC by means of identifying distinct sedimentary targets (e.g. basin outlet, the different stream systems over the course of the year, to a greater or lesser extent, and *lameiros*). Results are analysed in terms of geospatial variability and the role played by each factor, and discussed on the basis of the existing literature about soil erosion/deposition in *lameiros*. This study does not attempt to demonstrate that *lameiros* are sedimentation-prone areas, because this is something known, but to identify, simulate and map the months during which sediment gain or loss is the predominant process. These tasks have never been done, and thus, our study contributes with new data, maps and interpretation of the role played by *lameiros* in headwater catchment areas. This study also improves the understanding of soil redistribution processes in Mediterranean humid mountain areas of high ecological value, and at the same time anthropized, and affected by recurrent forest fires.

2. Material and methods

2.1. Study area

Two small headwater basins located in the transboundary zone between the Spanish province of Zamora and the Portuguese district of Bragança, were selected (Fig. 1a). The basins refer to the Candanedos Stream Basin (so-called in previous studies as 'Lave20_08', and in this study as B.08; 14.54 km^2) and the Ribera or Sil Stream Basin ('Lave20_13' in previous studies, and B.13 hereinafter; 17.23 km^2). Both streams converge at the same point (41° 54′ 48″ N, 6° 39′ 45″ W) giving rise to the Igrejas River. This hydrological aspect defines the extension of

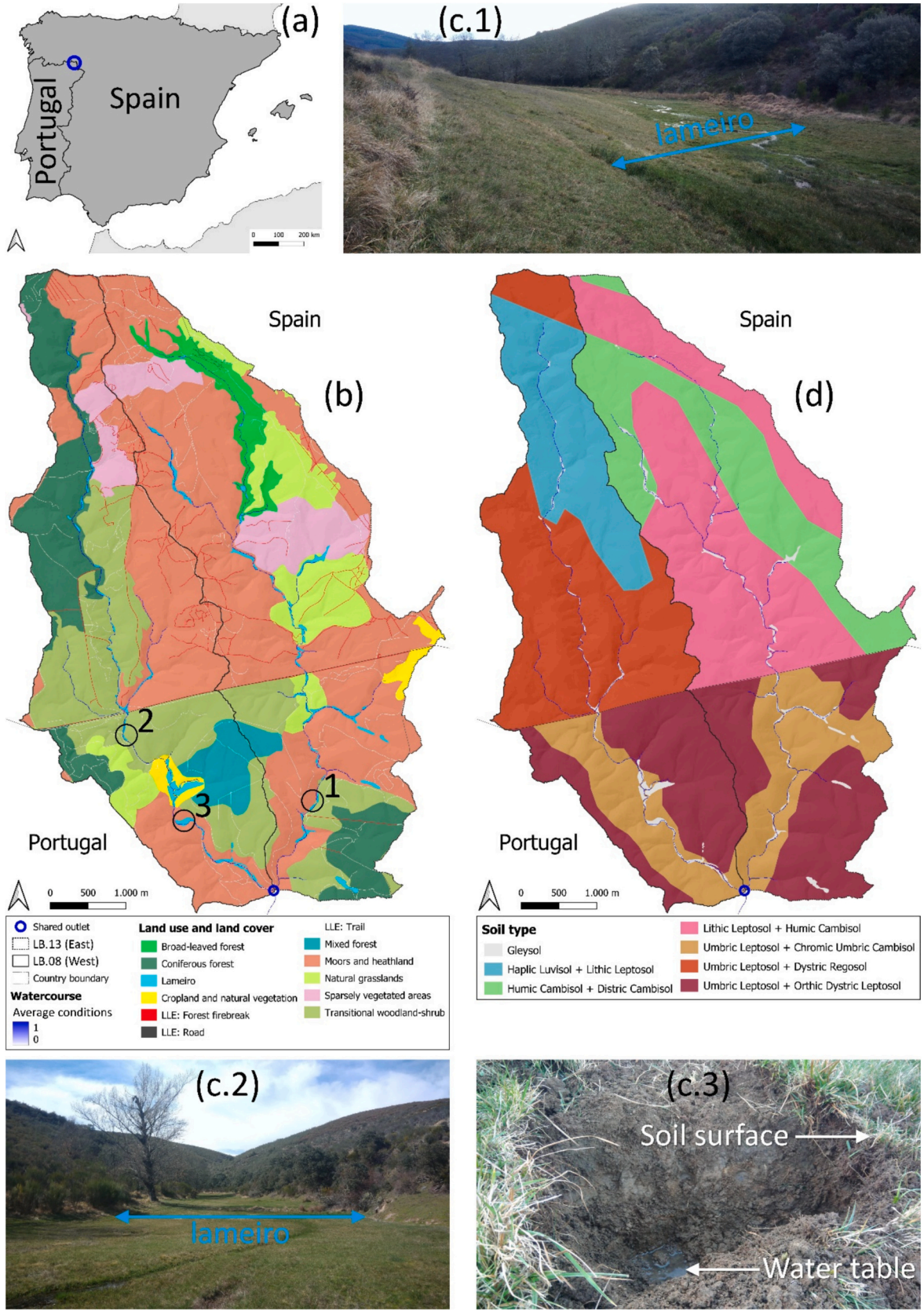

Fig. 1. Location of the study area (blue circle) in northern Portugal and north-western Spain (a). Map of the twelve land uses, including the linear landscape elements: Firebreaks, unpaved forest trails, and forest roads (b). Pictures (taken in February 26th 2019) of the abandoned *lameiro* with stream (c.1), in use *lameiro* with stream (c.2) and in detail in a pit showing the water table level in an in use *lameiro* with stream (c.3). Map of the seven soil types (d).

the two basins: from the point of confluence upstream. In both basins, the main drainage direction is from north to south, so that the highest elevations are in Spain, at 1084.9 and 1067.3 m a.s.l. in B.08 and B.13, respectively, and the point of confluence between the basins is located in Portugal at 686.6 m a.s.l. Both basins share one of the north-south divisions, being B.08 located to the west of the common division and B.13 to the east of it. The area located in Portugal is under environmental protection, being a part of the Montesinho Natural Park in the Trás-os-Montes region. In the last two decades, forest fires have affected study area. Between the years 2002 to 2004 and 2014 to 2011, there was a marked loss of vegetation (4.3 km^2), which indicated poor land management and a large number of fires. In 2017, a landmark year of forest fires in Portugal (Rodrigues et al., 2022), in contrast, in the study area, there was little vegetation loss –concentrated in the northern third of the study area, and affecting 116.6 ha (3.7 % of the total area).

A total of 12 land uses, including all *lameiros*, were mapped by means of combining different data sources like a recent orthomosaic from the Spanish institute of geography (PNOA, 2020), the most recent map of European Commission CORINE Land Cover (CLC) 2018 (Kosztra et al., 2019; EEA, 2020) and the Portuguese 'Carta de Uso e Ocupação do Solo' for 2018 (COS; DGT, 2018) (Fig. 1b). It should be noted that these two digital maps are after the sequence of fires described above, reflecting the changes that the fires produced in the vegetation. The CLC2018 map includes 8 land uses, and COS covers the Portuguese part of the research and provides more specific details, particularly regarding *lameiros*. Due to the relevance of these detailed *lameiros* data found in COS, they were adopted as a reference and replicated in the Spanish part of the study to ensure consistency and comparability between both regions, contributing to a robust and coherent analysis of land use throughout the study's context. Besides, linear landscape elements (unpaved forest trails, paved mountainous roads, and firebreaks) were mapped from PNOA. Most of the study area (45 %) is occupied by Moors and heathland, mainly in B.13 (54 %), which includes natural areas of spontaneous, sparsely or very dense vegetation (heather, briars, broom, gorse, laburnum, etc.) (Table 1). Transitional woodland-shrub refers to transitional bushy and herbaceous vegetation with occasional scattered trees, occupying 18 % with greater predominance in basin B.08 (31 %), as well as Coniferous forest (12 %) that occupies a larger surface area in B.08 (19 %). Next 9 % and 7 % are Natural grasslands (under no or moderate human influence, located on hilly terrain and steep slopes) and Sparsely vegetated areas (with little vegetation (10–50 %) composed of herbaceous and/or woody species and the rest with bare soil), respectively.

Lameiros are distributed in both the Spanish ($n = 56$) and Portuguese ($n = 43$) parts, being larger in the southern half and in B.13, with a similar number in the two basins: 51 and 48 *lameiros* in B.08 and B.13, respectively (Fig. 1c; more pictures in Supplementary Fig. 1). The mean ($\bar{x}$) and median ($\tilde{x}$) size is of the same order of magnitude in B.08 ($\bar{x} = 3056$ m^2; $\tilde{x} = 1240$ m^2) and B.13 ($\bar{x} = 4438$ m^2; $\tilde{x} = 2318$ m^2). *Lameiros* were classified into four types based on two criteria, use and water availability: i) in use with stream (17 and 0 in B.08 and B.13); ii) in use without stream (0 and 4 in B.08 and B.13); iii) abandoned with stream (31 and 41 in B.08 and B.13); and iv) abandoned without stream (3 in B.08 and B.13). With regard to water availability, two alternatives were found: i) well-irrigated (48 and 41 in B.08 and B.13), near permanent streams, usually in the bottom valley and middle slopes; and ii) poor-irrigated (3 and 7 in B.08 and B.13), along non-permanent or shallow watercourses, with small water sources, normally in valley bottoms, middle slopes and some plateaus.

Artificial landscape elements include 46 unpaved forest trails, well distributed in both basins, with total and average lengths of 119,595 and 316 m (density of 3208 m ha^{-1}). The paved mountainous roads add 7323 m length (density of 2289 m ha^{-1}) which are located in the northeastern part of B.13. Finally, 231 firebreaks appear throughout the two basins, with a total and average lengths of 64,340 and 279 m (density of 308 m ha^{-1}), which are mostly located in the Spanish part.

Topography is hilly and undulating, with a mean slope gradient (S) of 20.6 % and 19.4 % in B.08 and B.13, respectively. Very steep conditions ($S > 40$ %) only affect 8 % and 6 % of the surface of B.08 and B.13. Despite these general conditions, which are the predominant in the mid-mountainous areas of the Iberian Peninsula, moderate mean ($\bar{x}$) slope gradients appear in the *lameiros* ($\bar{x} = 11.1$ % in B.08, and $\bar{x} = 12.5$ % in B.13) and firebreaks ($\bar{x} = 11.9$ % in B.08, and $\bar{x} = 11.5$ % in B.13). The region's climate is Mediterranean temperate with continental influence (Csb according to the Köppen-Geiger Climate Classification). There is a 3-month rainy period (mean rainfall depth of 95 mm per month), between October and December, a 4-month humid period between January and April (77 mm per month) and a 5-month dry period between May and September (28 mm per month) with very low rainfall in July and August (<15 mm per month) (Charraza, 2011). The mean annual temperature of the air is 12.1 °C. The mean annual precipitation is around 733 mm (data source: Duero River water authorities – CHDuero; 'Tera en Puebla de Sanabria' weather station).

Table 1
Mean values of the main topographic parameters and inputs (S: slope, C: land use, cover and management factor, RT: roughness of the terrain, Kp: soil permeability, and FL: flow length) of the AIC for each land use in the two basins (B.08 and B.13). LLE: Linear landscape element.

CORINE	Land use and land cover	B.08 (Western part)						B.13 (Eastern part)						C
Code	Type	Area (%)	Elevation (m)	S (%)	RT (0–1)	Kp (0–1)	FL (m)	Area (%)	Elevation (m)	S (%)	RT (0–1)	Kp (0–1)	FL (m)	(0–1)
122	LLE: Unpaved forest trails	0.9	834.4	16.0	0.9477	0.7924	5777	0.9	868.7	14.5	0.9779	0.6072	6352	1.0000
122	LLE: Paved mountainous roads	–	–	–	–	–	–	0.1	902.6	18.4	0.9461	0.5407	8277	1.0000
243	Cropland with natural vegetation	1.4	732.0	24.0	0.9572	0.8166	3302	1.1	848.4	10.8	0.9803	0.7086	5472	0.1342
311	Broad-leaved forest	–	–	–	–	–	–	5.0	885.0	28.4	0.9520	0.4541	9264	0.0013
312	Coniferous forest	19.4	807.4	21.9	0.9733	0.7674	8602	5.2	800.0	23.4	0.9734	0.8159	2344	0.0011
313	Mixed forest	5.0	790.5	16.5	0.9790	0.8113	3690	0.9	836.8	13.1	0.9829	0.8113	3020	0.0011
321	Natural grasslands	3.0	810.0	26.6	0.9720	0.8240	4020	13.3	851.2	19.1	0.9764	0.4849	6880	0.0491
322	Moors and heathland	33.8	852.6	20.6	0.9744	0.7935	6387	54.0	852.7	19.4	0.9767	0.5550	6514	0.1000
324	Transitional woodland-shrub	30.8	892.4	20.4	0.9694	0.7971	5302	8.0	834.3	14.6	0.9788	0.8112	2912	0.0500
324	LLE: Forest firebreaks	1.0	887.7	11.9	0.9837	0.7886	8151	1.0	876.6	11.5	0.9856	0.4615	7190	0.0500
333	Sparsely vegetated areas	3.6	897.4	19.5	0.9770	0.8996	9631	9.2	873.4	19.1	0.9764	0.4630	7906	0.4500
411	Lameiros	1.1	732.3	11.3	0.9485	0.2155	3675	1.2	784.4	13.2	0.9482	0.1930	5166	0.0010

2.2. Index of sediment connectivity and simulated scenarios

For this study, the aggregated index of runoff and sediment connectivity (AIC) was used to calculate and map sediment connectivity. AIC was developed by López-Vicente and Ben-Salem (2019) on the basis of the previous equations by Borselli et al. (2008) and Cavalli et al. (2013). This index is a suitable approach to study structural and functional sediment connectivity at a variety of spatial and temporal scales (López-Vicente et al., 2020; Wu et al., 2023). This index combines the downward potential for the direction of flow occurring uphill ($\boldsymbol{D_{up}}$ component), and the probability of runoff and sediment reaching a sink along the flow path ($\boldsymbol{D_{dn}}$ component):

$$AIC_k = log_{10}\left(\frac{D_{up,k}}{D_{dn,k}}\right) = log_{10}\left(\frac{\overline{R_t} \bullet \overline{RT} \bullet \overline{C_t} \bullet \overline{K_P} \bullet \overline{S} \bullet \sqrt{A_k}}{\sum_{k=i}^{n} \frac{d_i}{AWC_i}}\right) \quad (1)$$

where subscript $\boldsymbol{k}$ indicates that each cell has its own AIC-value which is calculated on the basis of the above equation; $\boldsymbol{R_t}$ is the normalized rainfall erosivity factor for the period $\boldsymbol{t}$; $\boldsymbol{RT}$ is the roughness of the terrain factor; $\boldsymbol{C_t}$ is the vegetation and cropping management factor (RUSLE) for the period $\boldsymbol{t}$; $\boldsymbol{K}_p$ is the soil permeability factor; $\boldsymbol{S}$ is the slope gradient factor ($m \cdot m^{-1}$); $\boldsymbol{A}$ is the upward drainage area (m^2), $\boldsymbol{d_i}$ is the distance of the flow path at each pixel $\boldsymbol{i}$ (m); $\boldsymbol{n}$ is the total number of pixels that sediment travels from its source area to the defined sink; and $\boldsymbol{AWC}$ is the aggregate weighting factor:

$$AWC_i = R_{ti} \bullet RT_i \bullet C_{ti} \bullet K_{Pi} \bullet S_i \quad (2)$$

The values of the different inputs in the $\boldsymbol{D_{up}}$ component correspond to the average values of the upslope drainage area at each pixel. All input parameters in AIC have normalized values between 0.001 or 0.005 and 1 (for more details about index setup see López-Vicente et al., 2021).

In this study, three different computational targets were selected, with the aim of evaluating the process of sediment delivery/storage on different landscape features, namely: I) the shared outlet of the two basins (AIC-out); II) the watercourse (AIC-wc); and III) the *lameiros* (AIC-lam). AIC-out evaluates the sediment dynamic with temporal storage of sediment along the stream systems, because the stream system is simulated as hillslopes. AIC-wc considers sediment dynamic with no temporal storage of sediment, and thus, all sediment that reaches the stream leaves the basin. Additionally, and taking into account that the study area is located in two headwater basins (low flow) with marked seasonal variations in rainfall depth and erosivity, we distinguished and mapped three watercourses, one per erosive period: minimum (dry months with low erosivity), average (humid months) and maximum (rainy months with high erosivity) extension of watercourses. Finally, AIC-lam is focused on the role played by *lameiros* as sediment-sink areas. Therefore, 12 scenarios were computed: three of structural connectivity (AIC_{str}) and nine of functional (AIC_{fun}) connectivity (Table 2).

2.3. Data acquisition and index setup

The freely available airborne LiDAR (Light Detection and Ranging)-derived digital elevation model (DEM) provided by the Spanish National Centre for Geographic Information (IGN) was used in this study, corresponding to the first series (flight made in 2010). The DEM has a horizontal resolution of 5 × 5 m and provides elevation values with millimeter precision. The vertical accuracy of the LiDAR data is typically RMSE (Root Mean Square Error) ≤ 20 cm, while the horizontal accuracy is RMSE ≤30 cm. To ensure the continuity of the overland flow pattern, all artificial sinks, associated with minor local topographic depressions of a few millimeters deep, were filled. The new surfaces had a minimum gradient of 0.01°. The topographic inputs, $\boldsymbol{RT}$, $\boldsymbol{S}$ and $\boldsymbol{A}$ in Eqs. (1) and (2), were derived from the corrected DEM (Fig. 2a, b). $\boldsymbol{RT}$ was calculated as the inverse values of the standard deviation map of the slope gradient

Table 2
Simulated scenarios of structural and functional sediment connectivity considering different targets and erosive periods.

Target	Sediment connectivity			
	Structural	Functional		
	Annual average	High erosivity (Oct.–Dec.)	Moderate erosivity (Jan.–Apr.)	Low erosivity (May–Sep.)
Outlet	AIC_{str}-out	AIC_{fun}-outHE	AIC_{fun}-outME	AIC_{fun}-outLE
Watercourse – maximum extension	NC	AIC_{fun}-wcHE	NC	NC
Watercourse – average extension	AIC_{str}-wc	NC	AIC_{fun}-wcME	NC
Watercourse – minimum extension	NC	NC	NC	AIC_{fun}-wcLE
Lameiros	AIC_{str}-lam	AIC_{fun}-lamHE	AIC_{fun}-lamME	AIC_{fun}-lamLE

NC: No computation.

map. All inputs were prepared and outputs generated at 5 × 5 m of pixel size, and the geospatial computation was done using the tools (e.g. weighted flow length and flow accumulation with the Deterministic Infinity (D-Inf or D∞) algorithm) available in *QGIS Desktop 3.26.3* and *ArcGIS© Pro 3.1.2* software.

To calculate $\boldsymbol{R_t}$, Eq. (3), it was necessary to obtain the rainfall erosivity factor at the annual (R) and monthly (EI_{30}) scales, which was estimated using the data of precipitation of 9 hydrological years (from October 2012 to September 2021) recorded in the 'Tera en Puebla de Sanabria' weather station (data source obtained upon request: Duero River water authorities, CHDuero). This weather station (42° 03′ 30″ N, 6° 37′ 50″ W) is located 13 km northeast of the geographic center of the study area. As precipitation was recorded at daily scale, we used the approach developed by de Santos Loureiro and de Azevedo Coutinho (2001) in Portugal to estimate R with daily values of rainfall depth and tested successfully in Italy (Diodato, 2004) and Spain (López-Vicente et al., 2011): data source:

$$R = \frac{1}{N}\sum_{m=1}^{12}\left(7.05 \bullet rain_{m10} - 88.92 \bullet days_{m10}\right) \quad (3)$$

where $\boldsymbol{N}$ is the number of years, $\boldsymbol{m}$ is the month, $\boldsymbol{rain_{m10}}$ is the monthly rainfall ≥10 mm, $\boldsymbol{days_{m10}}$ is the monthly number of days with rainfall ≥10 mm. For this 9-year period, the average ($\overline{x}$) R value was of 1280 MJ mm/ha h yr ($\boldsymbol{R_t} = 1.0$), where unit 'h' denotes hours. When $\boldsymbol{m}$ represents a specific month, then the result of Eq. (3) is the EI_{30} value of that month. After calculating EI_{30}, the mean rainfall erosivity was obtained for each erosive period: 645, 458 and 177 MJ mm/ha h month for the highly (from October to December), moderately (from January to April) and low (from May to September) erosive period, respectively. Besides, the $\boldsymbol{R_t}$ factor, see Eqs. (1) and (2), of each period was calculated: 0.504, 0.358 and 0.138 (more details in Supplementary Table 1). As we only have data from one weather station, we used one unique value of $\boldsymbol{R_t}$ for each period for the whole study area. Further research should consider the installation of additional weather stations within the basins that would allow mapping $\boldsymbol{R_t}$ in a spatially distributed way.

The values of the C-factor, representing the capacity of different land uses to mitigate soil erosion (as presented in Table 1), were derived from synthesis studies conducted by Panagos et al. (2015) for European Union countries and by Marques et al. (2021) specifically for Portugal. While it is acknowledged that vegetation cover in certain plants may vary throughout the year, such as broadleaf species shedding leaves during the winter or cereal fields having short harvesting cycles, the decision was made to keep the C-factor values constant throughout the three

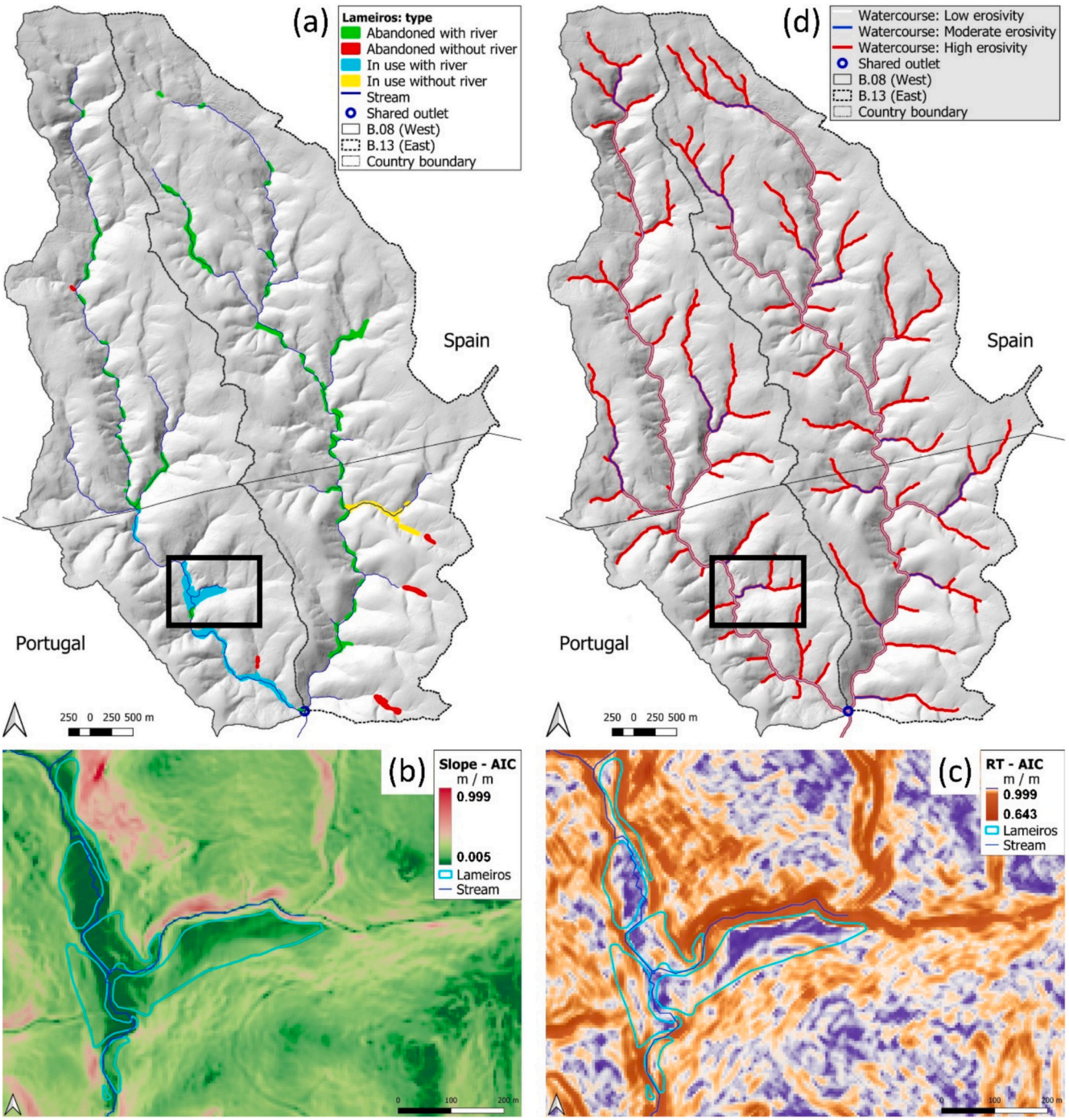

Fig. 2. Spatial location of the four types of *lameiros* (a) and of the three watercourses associated with the three erosive periods: High erosivity (Oct.–Dec.), moderate erosivity (Jan.–Apr.), and low erosivity (May–Sep.) (d). Zoom-in view of the maps of the slope gradient (b) and roughness of the terrain (c) factors in an area surrounding *lameiros*.

erosive periods of the year. This choice was made to simplify the sediment connectivity index calculation and avoid introducing additional variability into the results. Although meadow vegetation like that in *lameiros* may exhibit seasonal variation, particularly in the spring (Pereira and Arrobas, 2010), this variation does not appear to be significant enough to substantially influence the results of soil erosion and sediment transport. This fact is especially relevant because the percentage of soil cover in the four types of *lameiros* in this study area is the same and near 100 % and remains constant throughout the year. Therefore, the use of annual C-factors is opted for in this study as a more appropriate and representative approach to the prevailing conditions of the *lameiros* in question.

Due to the shared boundaries of the basins spanning two countries, a consolidation of data from both nations was undertaken to generate soil maps, resulting in the identification of seven combinations encompassing nine distinct soil types and the incorporation of the ***Kp*** factor (Fig. 1d). Data of soil permeability pertaining to the Portuguese and Spanish territories were made available by the National Geographic Information System (SNIG) of Portugal and the Geological and Mining Institute of Spain (IGME), respectively (Supplementary Table 2). To ensure compatibility and standardization of nomenclature, we relied upon the research conducted by de Figueiredo (2013) and the references

from Agroconsultores and Coba (1991), which are grounded in the classification framework of the Food and Agriculture Organization (FAO, 1981).

By using GIS tools (aerial orthophotos and the overland flow pathways) and after identifying in the field the beginning of the streams during the different erosive periods, the masks that correspond to the three watercourses were generated (Supplementary Table 3) and used as targets for computing the three maps of functional connectivity associated with the watercourses: AIC_{fun}-wcHE, AIC_{fun}-wcME and AIC_{fun}-wcLE (Fig. 2d). The total length of the streams for the HE, ME and LE scenarios were 88,665, 39,310 and 27,555 m, respectively. IC and AIC use masks with binary values (0 or 1), that modify the flow direction map, to simulate the sediment connectivity process considering the pixel as part of the slope (value equal to 1) or part of the target (value equal to 0). For AIC-out, watercourses had value equal to 1 (sediment storage in the watercourses), for AIC-wc, watercourses had value equal to 0 (net sediment export outside the basins), and for AIC-lam, the value 0 was associated with the *lameiros*, in order to consider this feature as a sedimentation-prone area.

2.4. Statistical analysis and index performance

All maps were analysed using geo-statistical tools available in *ArcGIS© Pro 3.1.2* and *QGIS 3.26.3* considering the two basins independently. We did it in this way because the areas, polygons in GIS, of each land use are located at distinct distances with respect to the five computational targets within each basin, and thus, the role played by each land use on AIC was slightly different. Besides, the physiographic characteristics (slope degree, roughness of the terrain, flow length) also differ a little among basins. The analysis of the maps of the twelve scenarios (Table 2) included the corresponding maps of percentiles, with special attention to the lowest (<10th (P10) percentile) and highest (>90th (P90) percentile) connectivity. Besides, we analysed how the spatial location of these areas changed among scenarios. The percentile maps were obtained using the histogram of each AIC map and GIS tools.

The available literature about soil depth at the hillslope scale and within the *lameiros*, as well as about the soil physical and chemical properties of the *lameiros*, was used to discuss the role of this landscape feature as depositional-prone areas. On the other hand, the use of models to evaluate sediment transport in ungauged basins is a challenge, due to the difficulty of validating the results with independent metrics. Therefore, it is necessary to choose a model previously tested in physiographic conditions similar to those of the study area. The predictive capacity of IC and AIC in studies of sediment delivery has been probed in different areas of Spain and Portugal by several authors, by means of validation with measured rates of sediment yield and stream flow, in studies of structural and functional connectivity, such as in mountainous landscapes by Abebe et al. (2023) and Wu et al. (2021), in fire-affected areas López-Vicente et al. (2021), and with marked land use changes (González-Romero et al., 2021, 2022). Abroad Mediterranean countries, both indices have been successfully tested like in China (Wu et al., 2023) and Japan (López-Vicente et al., 2017). Therefore, we consider the AIC results in this study to be reliable. On the other hand, most of the small mountain basins around the world are not gauged, and the use of models in a GIS environment provides useful information, most of the time unpublished, to understand the sedimentological functioning within these areas.

3. Results

3.1. Structural sediment connectivity

The three maps of structural sediment connectivity show, for the first time in the literature, the conditions of potential sediment transport, temporal accumulation and sedimentation that happen in the studied basins with especial focus on the role played by *lameiros*. The map of AIC_{str}-out showed the probability of sediment delivery during dry conditions (e.g. drought periods) when overland flow is limited to the streams, with minimum flow, and their surrounding areas (Fig. 3a).

The map of AIC_{str}-wc (Fig. 3b) represented the conditions during wet/rainy periods, in which three processes take place: I) the whole basin is active (runoff is generated and flows over the entire surface), and thus, there is a net sediment supply from the slopes to *lameiros* (high sediment accessibility and high availability), II) the sediment that reaches the stream leaves the study area and therefore there is a net loss of soil; and III) *lameiros* acted as sedimentation-prone areas (moderate sediment accessibility and high availability) with lower values of connectivity (−7.0 % and −5.1 % in B.08 and B.13) than that at the basin scale (Fig. 3e).

The map of AIC_{str}-lam was focused on the role played by *lameiros* as sinks of sediment that comes from the slopes (lateral connectivity) and streams (Fig. 3c). This element of the landscape presents unique characteristics, due to its location at the bottom of the valleys (areas of very low slope next to or between water courses), due to the human activity that defined its geometry in the past, and due to its regulatory role in surface hydrology and temporary sediment storage. From a sedimentological point of view, *lameiros* can be considered as silted wetlands or clogged ponds. In AIC_{str}-lam, each *lameiro* acted as a sediment sink for the eroded soil coming from the corresponding upslope drainage area.

Due to the configuration of the index, and its dimensionless nature, the value in each pixel depends on the target chosen in each simulation. These aspects explain the distinct mean ($\overline{x}$) and standard deviation (σ) values obtained in the three maps of structural sediment connectivity for each basin: AIC_{str}-out (B.08: $\overline{x} = -10.030$ and $\sigma = 1.069$; B.13: $\overline{x} = -9.327$ and $\sigma = 1.015$) AIC_{str}-wc (B.08: $\overline{x} = -6.808$ and $\sigma = 1.667$; B.13: $\overline{x} = -6837$ and $\sigma = 1.578$) AIC_{str}-lam (B.08: $\overline{x} = -7.382$ and $\sigma = 1.515$; B.13: $\overline{x} = -7.076$ and $\sigma = 1.338$); as well as the different spatial patterns and distribution of maximum and minimum values. In the B.08 basin, a limited sediment transport capacity was evident in areas predominantly covered by coniferous forests (see map of Fig. 1b), as inferred from the P10 (10th percentile) values, which exhibited a uniform distribution in the AIC_{str}-out, AIC_{str}-wc and AIC_{str}-lam maps (Fig. 4a). In contrast, in the B.13 basin, the distribution of P10 values occurred more diffusely, although there was a slight concentration in the south-western region, characterized by the predominance of coniferous forests (Supplementary Fig. 3). Notably, the AIC_{str}-lam map in B.13 revealed a considerable amount of P10 values in the eastern part, where mixed forest areas were found, suggesting relatively reduced sediment connectivity even in these contexts. In B.08, the AIC_{str}-wc and AIC_{str}-lam maps showed a similar trend, with more pronounced P90 (90th percentile) values in the central and southern parts of the basin, near watercourses, indicating high sediment connectivity in these areas, where sediment discharge from the basin occurs. Additionally, P90 values were more prominent in transitional woodland-shrub and moors and heathland. However, in the AIC_{str}-lam map of B.08, P90 values were more dispersed, covering areas of transitional woodland-shrub, mixed forest, and cropland with natural vegetation.

3.2. Functional sediment connectivity

The maps of functional connectivity associated with the outlet (AIC_{fun}-outHE, AIC_{fun}-outME, AIC_{fun}-outLE) and *lameiros* (AIC_{fun}-lamHE, AIC_{fun}-lamME, AIC_{fun}-lamLE) showed the same spatial pattern of those maps of AIC_{str}-out and AIC_{str}-lam, but with different values of connectivity due to the effect of the seasonal changes of the rainfall erosivity factor, R_t in Eqs. (1) and (2). Therefore, the spatial location of the lowest (P10) and highest (P90) values of connectivity (Supplementary Fig. 4a, b) was the same between AIC_{str}-out and AIC_{fun}-out, and between AIC_{str}-lam and AIC_{fun}-lam. In the case of functional connectivity associated with the watercourse (AIC_{fun}-wcHE, AIC_{fun}-wcME, AIC_{fun}-wcLE), the three maps showed different spatial patterns owing to the different configuration of the index with the short, medium and large

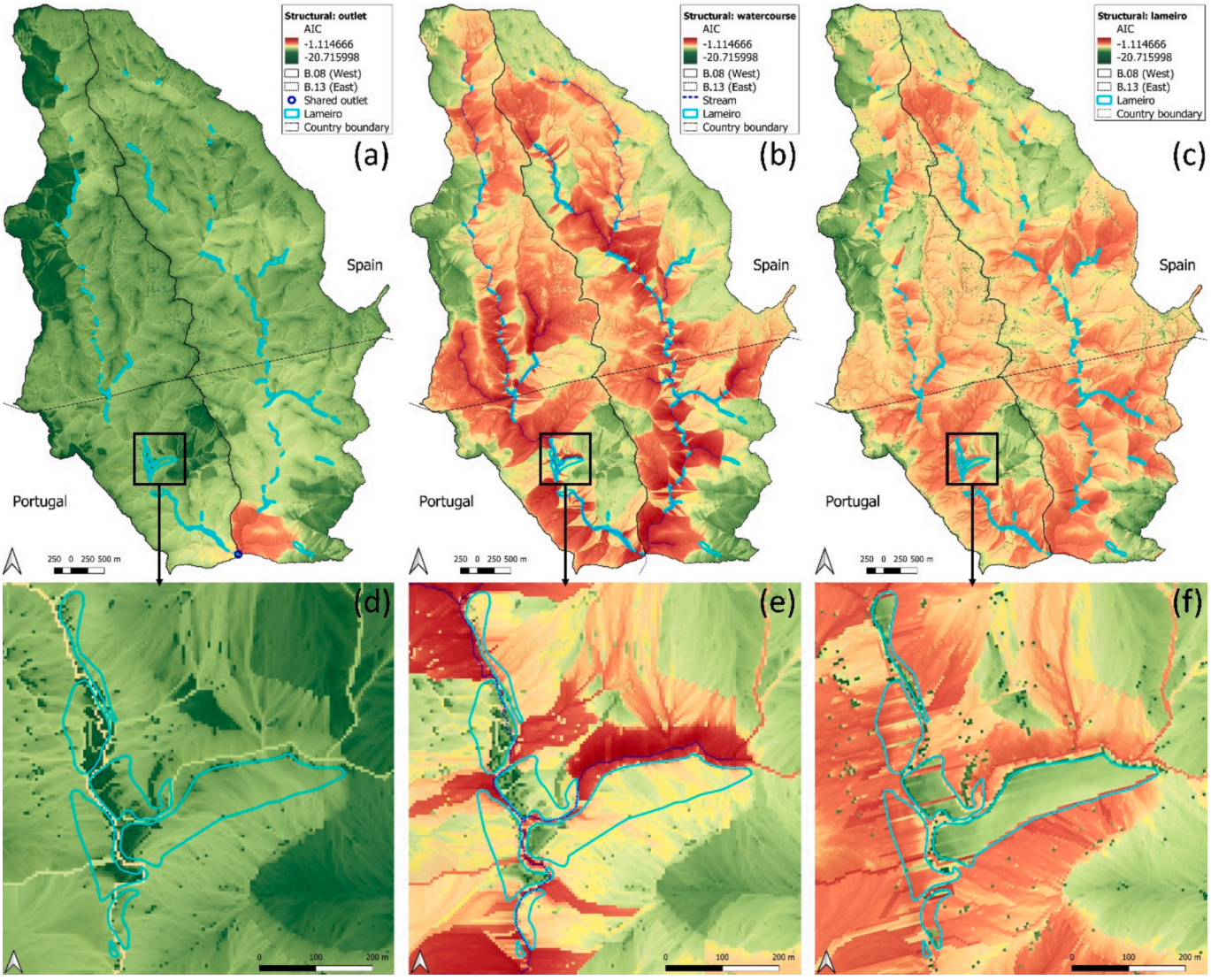

Fig. 3. Maps of structural sediment connectivity (AIC_{str}) of the two basins using the outlet (a), watercourse (average extension, see Table 2) (b) and lameiros (c) as computational target (red colours indicate high connectivity and green colours indicate low connectivity). Zoom-in view near the lameiros (boundary in light blue) of the three maps, showing the dis-connected areas (dark green) (d, e and f).

stream system, which reflected low, moderate and high rainfall erosivity, respectively. Considering the two basins, the mean value of AIC_{fun}-outHE, AIC_{fun}-outME, AIC_{fun}-outLE was 6.6 %, 9.8 % and 18.1 % lower than that of AIC_{str}-out, in a way imitating the differences in rain erosivity between the three periods and the annual erosivity (−50 %, −64 % and −86 %).

In the case of AIC_{fun}-lam, the three maps (HE, ME and LE) had mean values, considering the two basins, that were 8.2 %, 12.4 % and 23.8 % lower than the mean value of AIC_{str}-lam; these differences being associated only with the configuration of the index and the values of the rain erosivity factor. When *lameiros* were the computational target, the differences between the functional and structural connectivity were more marked than in the case of AIC-out.

In the case of the three maps of functional sediment connectivity associated with the watercourses, the spatial patterns differed to a greater degree due to the combined changes in rainfall erosivity and the extension of the watercourses network (Fig. 5). For the two basins, the mean value of AIC_{fun}-wcHE, AIC_{fun}-wcME and AIC_{fun}-wcLE was 3.1 % higher and 12.8 % and 30.7 % lower than that of AIC_{str}-wc. Comparing the AIC_{fun}-wc percentile maps (Supplementary Fig. 4c) with the corresponding AIC_{str}-wc map (Supplementary Fig. 3), moderately different spatial patterns can be seen in the AIC_{fun}-wcLE and AIC_{fun}-wcHE maps, while the pattern of AIC_{fun}-wcME was the same as that of AIC_{str}-wc, but with different values (the stream mask used in AIC_{str}-wc was the same as that used in AIC_{fun}-wcME).

Despite the different sedimentological meaning of the AIC_{fun}-out, AIC_{fun}-lam and AIC_{fun}-wc maps, the effect of the three erosive periods was similar in the various land uses in each basin, following a decreasing sequence: HE > ME > LE (Fig. 6). In the individual analysis of Fig. 6a, which refers to AIC_{fun}-out, in the average values, transitional woodland-shrub in B.13 showed higher AIC values. Considering the minimum AIC values in B.13, higher connectivity was associated with *lameiros*, natural grasslands, and moors and heathland. In B.08, the lowest values corresponded to coniferous forest, *lameiros* and sparsely vegetated areas, respectively. During the most erosive period (HE), *lameiros* registered the lowest AIC value in B.13 and the second lowest value in B.08, highlighting the significant relevance of this land use in hydrological connectivity. As for AIC_{fun}-lam (Fig. 6b), moors and heathland (LULC.09) and *lameiros* in both basins and paved mountainous roads in B.13 stands out at the highest values. The prominent presence of LULC.09 in high connectivity areas can be attributed to its direct connection to the object of calculation in this scenario. In Fig. 6c,

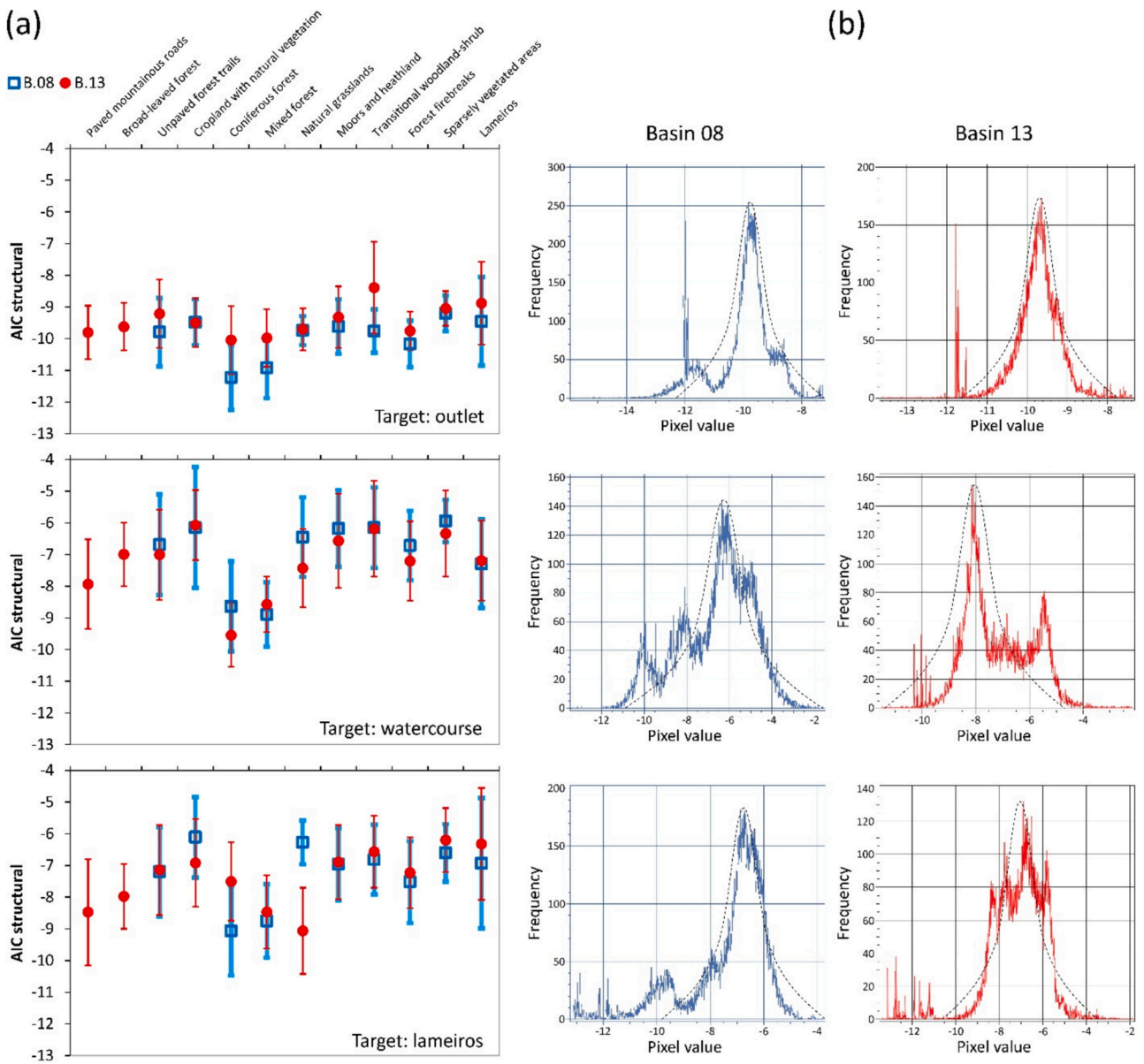

Fig. 4. Mean and standard deviation values of structural sediment connectivity (AIC_{str}) for each land use at the two basins with the three computational targets (a). Histograms of the three maps of AIC_{str} generated at each basin, and Gaussian-type curve, in dotted black line, that better fits the AIC value distribution (b).

referring to AIC_{fun}-wc and compared to the other scenarios, there was a trend towards higher minimum, maximum and average values throughout the erosion periods.

4. Discussion

4.1. Role of the outlet, watercourses and lameiros

Regarding the AIC_{str}-out map, which represents sediment delivery during dry conditions, the results indicate that under this scenario, which is less frequent than the humid one, the temporal storage of sediment is the predominant process in the stream system (González-Romero et al., 2021), sediment delivery is short (Cerdà et al., 2021) and similar to that observed in small basins without streams (López-Vicente et al., 2021). During dry periods, sediment supply from slopes to *lameiros* is very limited (low sediment availability and moderate sediment accessibility; see these concepts in Najafi et al., 2021), and *lameiros* act as sediment source areas of the temporally stored sediment that came during previous events (wet periods). Our results, with higher values of connectivity between the 99 *lameiros* and the basins' outlets (+6 % and +5 % in B.08 and B.13) than those of the remaining land uses with the outlets supported this hypothesis (high sediment accessibility and moderate availability) (Fig. 3d).

In contrast to the dry conditions represented by the AIC_{str}-out map, the AIC_{str}-wc map highlights sediment dynamics during wet/rainy periods in medium-size basins with a Mediterranean temperate climate. These basins are characterized by marked temporal fluctuations of river flow and sediment transport capacity, meaning that AIC_{str}-wc cannot be considered as the representative map of sediment connectivity during every day of the year. For this type of basins, the combined use of AIC_{str}-out and AIC_{str}-wc appears as the right choice to figure out the actual pattern of sediment storage and delivery over the course of the year (López-Vicente et al., 2020; Torresani et al., 2023), offering a complete view of sediment budget in ungauged basins. This double-target approach of sediment connectivity is also recommended in areas with strong seasonality of runoff and erosion dynamics (Souza and Hooke, 2021; Yan et al., 2022), and our study area presents marked seasonal changes on rainfall depth and erosivity. This characteristic of different

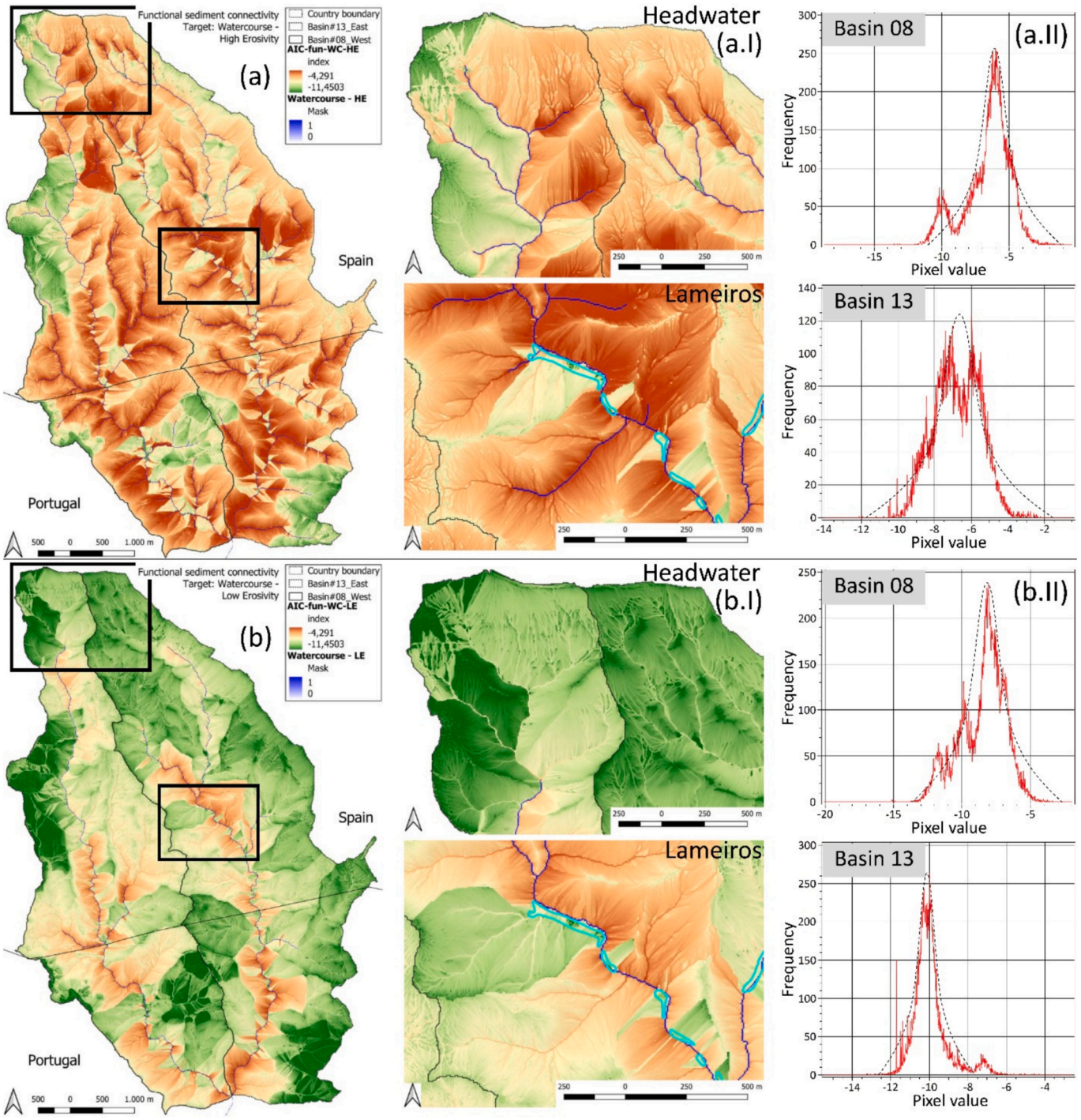

Fig. 5. Maps of functional sediment connectivity of the two basins using the watercourse as target (AIC_{fun}-wc) showing the two most contrasted watercourses: the large one and representative of high erosivity (a) and the short one and representative of low erosivity (b). The zoom-in views of the headwater area and near the *lameiros* (boundary in light blue) are also included (a.I and b.I). Right part of the figure: Histograms of the maps of AIC_{fun}-wcHE and AIC_{fun}-wcLE at each basin (a.II and b.II), and Gaussian-type curve, in dotted black line, that better fits the AIC value distribution.

sedimentary behaviour in the same landscape units throughout the year and during different erosive periods was already identified in mountain headwater basins in previous studies in areas with physiographic characteristics similar to those of our study (Alvera and García-Ruiz, 2000). In other areas, Colosimo and Wilcock (2007), López-Vicente et al. (2015) and González-Romero et al. (2022), also found periods or episodes with predominance of net soil loss or net soil deposition affecting the same landscape feature. As sediment supply conditions from slopes to *lameiros* predominate in this site against sediment source conditions from *lameiros* to streams, AIC identified *lameiros* as a sediment sink feature, which agrees with the geomorphological and soil evidences, and thus, our simulations were correct.

The AIC_{str}-lam map, which focuses on the role of *lameiros* as sediment sinks, allowed quantifying their role in the spatially distributed process of sediment delivery within the two basins. This map highlights how *lameiros* act as disconnecting elements of sediment transport from the upslope source areas to the outlet (Fig. 3f). Our results agreed with those reported by Fernandes (2019) who estimated an average soil depth of

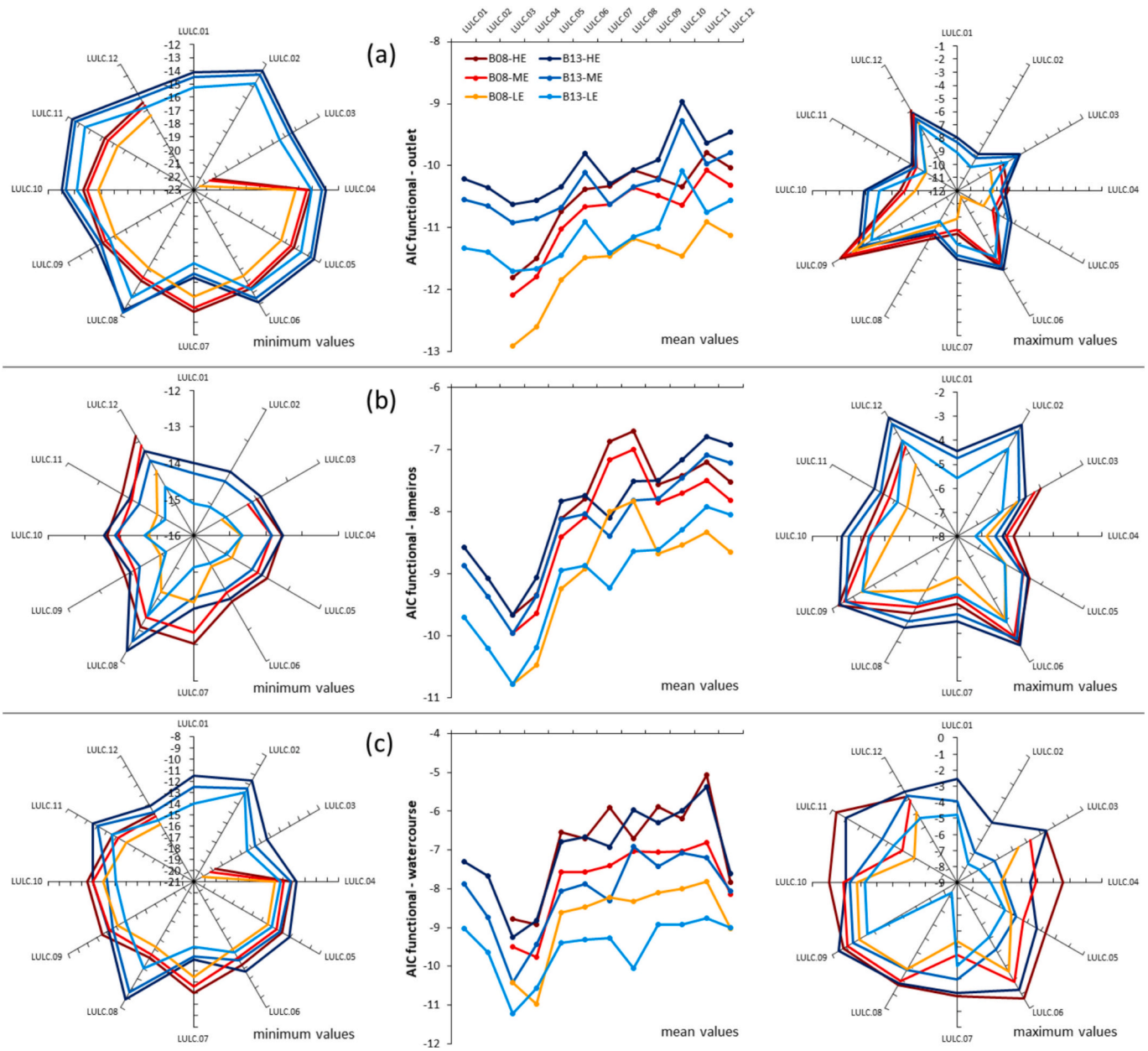

Fig. 6. Evolution of the values of functional sediment connectivity (AIC_{fun}) over the three erosive periods: HE (high erosivity), ME (moderate erosivity) and LE (low erosivity) at each land use and basin, considering the outlet (graphics on top), watercourse (graphics in the middle) and *lameiros* (graphics at the bottom). LULC.01: Broad-leaved forest; LULC.02: Paved mountainous roads; LULC.03: Coniferous forest; LULC.04: Mixed forest; LULC.05: Forest firebreaks; LULC.06: Unpaved forest trails; LULC.07: Natural grasslands; LULC.08: Cropland with natural vegetation; LULC.09: Moors and heathland; LULC.10: Transitional woodland-shrub; LULC.11: Sparsely vegetated areas; LULC.12: *Lameiros*.

40 cm in fifteen *lameiros* located in different areas within the Montesinho Natural Park (Supplementary Fig. 2), which indicated that *lameiros* are predominantly areas of sedimentation. In a more recent study carried out in four *lameiros* located in the southern part of our study area (one *lameiro* crossed by a stream and in use, one crossed by a stream and abandoned, one without stream and in use, and one without stream and abandoned) and using electrical resistivity tomography, Royer et al. (2020) found a significant accumulation of sediments in this element with deeper soils compared to the soils of the surrounding land uses (Supplementary Fig. 2). With a similar approach to our study, three targets: outlet, stream and a geomorphological sedimentation element, Cavalli et al. (2013) used a modified IC approach in the Italian Alps to evaluate sediment delivery with reference to the outlet, main streams and lakes, in order to refine the role played by lakes as sediment sinks. Further research will consider the use of the index of sediment connectivity together with a soil erosion model to quantify sediment yield to the *lameiros*, such as Duan and Li (2023) did in a large Chinese lake with the InVEST approach.

The analysis of the three maps of structural sediment connectivity (AIC_{str}-out, AIC_{str}-wc, and AIC_{str}-lam) reveals distinct patterns of sediment dynamics in the studied basins. As expected, the highest connectivity, and spatial variability, appeared in AIC_{str}-wc, whereas the lowest connectivity, and spatial variability, was found in AIC_{str}-out. Considering the contributing areas of *lameiros* (AIC_{str}-lam), the connectivity of this land use was 6 % (B.08) and 11 % (B.13) higher than that at the basin scale, highlighting the role played by this element with respect to the remaining land uses. These results were explained by the shorter distances from the hillslopes to the target in the case of AIC_{str}-wc, which

is distributed along the main bottom valleys, compared to AIC_{str}-out that is located at the point of lowest absolute elevation. Crema et al. (2015) in northern Italy, López-Vicente et al. (2020) in southeaster Spain and Yan et al. (2022) in central China also found similar results when compared maps of sediment connectivity generated for a specific site using different targets.

It should be noted that AIC_{str}-lam showed intermediate values of connectivity due to the scattered location of *lameiros* throughout the valleys of the two basins, highlighting the specific role played by this element that modifies the original patterns of soil loss, transport, deposition and yield, favouring sediment deposition within the basins. On the other hand, and although the influence of the size of the basin on the index values (González-Romero et al., 2021) and sediment transport (Parsons et al., 2006) are facts already demonstrated, this influence is not appreciated in this study due to the comparable size of both basins. This fact explained the lower average structural connectivity obtained in the abandoned and well-irrigated *lameiros* than that found in the in-use and poor-irrigated *lameiros* (Table 3).

The spatial distribution of P10 and P90 values in the AIC_{str} maps highlights the influence of land use and location on sediment connectivity in the studied basins. These results, on the one hand expected, reinforce the important role of factor C, or any other associated with the land use, on AIC values, as already demonstrated in previous studies with various proposals for the connectivity index (Hooke et al., 2021; Liu et al., 2022), and on the other hand, they highlight the importance of the location of the different land uses on the real impact that each use has on the value of the index. In a recent study using an artificial neural network in large Australian basins with multiple sub-catchments, Asadi et al. (2023) showed that the most effective parameters influencing the AIC values varied among different basins depending on their location and range of values.

In B.13, P90 values were mainly concentrated in the southern and central regions, particularly in moors and heathland and sparsely vegetated areas. In these areas, P90 values predominated, as well as in transitional woodland-shrub and moors and heathland. In both basins, the AIC_{str}-out map revealed a significant concentration of P90 values in the south, where transitional woodland-shrub moors and heathland predominate. This concentration of P90 values aligned with the study's findings by Yan et al. (2022), which showed that IC values tend to be higher when the channel network is used as a reference. This is due to the short distance between the slope areas and the main channels in the basins, which favours the rapid incorporation of sediment into the waterways. In B.13, this concentration extended slightly further to the north, following a trend similar to the AIC_{str}-wc map.

The combined analysis of the histograms (Fig. 4b), together with the mean values and standard deviation, provides a more comprehensive understanding of the behaviour observed in each scenario. The AIC_{str}-out histograms of the two basins showed a distribution similar to a Gaussian curve with the exception of a sharp peak in the lowest AIC values that corresponds to the coniferous forest located far from the main streams. This pattern was related to the way watercourses were considered in the analysis, simulating slopes in the terrain. On the other hand, in the AIC_{str}-wc histogram, where watercourses were treated as permanent, there was a noticeable component associated with net soil loss or sediment export. This resulted in a distinct pattern in the histogram, which was related to the different types of land use. In the AIC_{str}-lam histogram, the peaks associated with lower values were more frequent. This observation was mainly due to the more significant sediment accumulation in this specific land use, which acted as accumulation zones or sediment sinks. The predominance of these areas in both basins influenced the characteristic shape of the histogram, highlighting the influence of *lameiros*. These results contribute new information to the literature, constituting the first study that quantifies, spatially distributed, the role of *lameiros* as elements of sediment accumulation from slopes and water courses.

When these observations were related to flow length, it was possible to understand better how sediment transport distance affected sediment delivery in each scenario. In areas with shorter flow lengths, such as those related to coniferous forests, especially in B.13, there was rapid incorporation of sediment into streams and efficient export of sediment in the AIC_{str}-out and AIC_{str}-wc scenarios, respectively. This rapid incorporation reflected the high hydrological connectivity in these areas, in line with the studies by Wang et al. (2014).

Table 3
Mean value of structural sediment connectivity in the different types of *lameiros* in the two basins and considering the three computational targets (outlet, stream, and *lameiros*).

Lameiros	B.08			B.13		
	Outlet	Stream	*Lameiros*	Outlet	Stream	*Lameiros*
All (n = 99)	−9.45	−7.29	−6.93	−8.88	−7.19	−6.32
In use with stream (n = 17)	−9.33	−7.25	−7.01	nd	nd	nd
In use without stream (n = 4)	nd	nd	nd	−8.49	−6.81	−5.67
Abandoned with stream (n = 72)	−9.53	−6.69	−6.63	−9.09	−6.95	−6.42
Abandoned without stream (n = 6)	−9.01	−7.65	−5.61	−8.19	−7.76	−6.61

4.2. Role of the seasonal changes and land-use location

The analysis of functional connectivity maps (AIC_{fun}-out, AIC_{fun}-lam, and AIC_{fun}-wc) reveals the impact of seasonal changes in rainfall erosivity on sediment dynamics in the studied basins. In the specific context of AIC_{fun}-out, the presence of relatively high values in transitional woodland-shrub and moors and heathland zones—compared to other land uses—, regardless of seasonality, leads to more significant sediment transport outside the basins. This trend is especially evident when connectivity is assessed with respect to the catchment outlet, such as Cavalli et al. (2013) did in the Italian Alps and Llena et al. (2021) in the Spanish Pyrenees.

The observed differences in connectivity values between AIC_{fun}-lam and AIC_{str}-lam, particularly the lower mean values in the former, highlight the significant role played on the values of connectivity was more noticeable than in the case of the outlet that is a unique point or pixel. The spatial patterns of AIC_{str}-lam and AIC_{fun}-lam (HE, ME, LE) suggested that the impact of *lameiros* on sediment connectivity may be analogous to structures such as natural dykes or man-made check-dams, whose purpose is to retain sediment and control overland flow velocity and magnitude. This interpretation is supported by previous studies that have documented a significant reduction in sediment connectivity between the slopes and the streams following the implementation of sediment-retention structures, observed in basins impacted by forest fires in south-eastern Spain (Albert-Belda et al., 2019; González-Romero et al., 2022), and in a mountainous sub-basin in Calabria, southern Italy (Bombino et al., 2020). In the case of watercourses, the type of structures that would reduce sediment export would be dams, dikes or large check-dams (Terêncio et al., 2020; Galia et al., 2021).

The spatial and temporal variability in sediment connectivity, as evidenced by the differences in P90 values across the AIC_{fun}-wcHE, AIC_{fun}-wcME and AIC_{fun}-wcLE scenarios, underscores the significant role of seasonal variations in rainfall erosivity and watercourse dynamics. The highest dispersion of P90 values along the hydrographic network was present in the AIC_{fun}-wcHE scenario, followed by an intermediate concentration in AIC_{fun}-wcME and the highest spatial concentration of P90 values appeared in AIC_{fun}-wcLE, corroborating patterns observed by López-Vicente and Ben-Salem (2019) in a large basin in the Spanish Pyrenees with marked seasonal changes in stream

flow and sediment connectivity. The seasonal variation found in our study may indicate an increase in the water load for the channels, resulting in more significant sediment transport during the autumn (AIC_{fun}-wcHE) and winter (AIC_{fun}-wcME). These seasonal patterns are usually characterized by counterclockwise loops such as Buendia et al. (2016) found when studying temporal storage of sediment within the streams. This temporal dynamic can become very marked, especially under topographic conditions that favour the retention of sediment in the middle zones of the hydrological basin, and whose effective transport and export depends on variations in the water regime of the water courses, as Martini et al. (2022) observed in the Italian Alps.

Focusing on the extreme scenarios of high erosivity (AIC_{fun}-wcME) and low erosivity (AIC_{fun}-wcLE), as illustrated in Fig. 5a and b, the marked seasonal influence during the erosion periods is noticeable. A relatively normal distribution is observed when exploring the histogram during the most erosive period (AIC_{fun}-wcHE) in basin B.13. This consistency suggests that sediment connectivity maintains uniformity along the watercourses, which is crucial for understanding how water flows and interacts with the landscape, especially at critical times of erosion. In basin B.08, there are two peaks in the histogram. The higher peak shifted to the right, indicating areas with more intense connectivity, possibly related to significant erosion processes. The lower peak, in the centre of the scale, suggests areas with less connectivity. In the context of the AIC_{fun}-wcLE, the histogram in basin B.08, there are two smaller peaks, suggesting variations in connectivity along the watercourses. In basin B.13, the histogram is narrower, indicating less variation in AIC, but suggesting more uniform connectivity. However, there are two distinct peaks, suggesting occasional variations in connectivity. In both the AIC_{fun}-wcHE and AIC_{fun}-wcLE, lower values are located in *lameiros* (Fig. 5a.II, b.II), confirming the role of these areas in the control and barrier of sediment transport. Altogether, our results show the convenience of conserving and protecting –through some legal figure– the *lameiros* as active elements of the landscape that retain the sediment that comes from the slopes, regulating and reducing the export of sediment towards the main water courses, both within the basin as well as outside it.

In the transitional woodland-shrub area (B.13), the elevated AIC values can be attributed to its proximity to the calculation object, explained by its proximity to the object of calculation (Souza and Hooke, 2021), added to the high values of rainfall erosivity. The prominent presence of LULC.09 in high connectivity areas can be attributed to its direct connection to the object of calculation in this scenario. These results agreed with available studies, where roads are potential sediment transport routes (Alder et al., 2015; Nosrati and Collins, 2019) that contribute to the increase in AIC. This pattern was explained due to the drainage network used as a target, mainly due to the short distance between the slope areas and the catchment channels (Yan et al., 2022). However, in the minimum AIC values in both basins, LULC.03, LULC.12 and LULC.07 stand out. It is worth emphasizing the importance of *lameiros* (LULC.12), which, in addition to having a low C factor and, therefore, a high degree of protection against erosion, are directly connected to the object of calculation, playing a crucial role in protecting against the arrival of sediment in the drainage network.

Further research on the role of *lameiros* in soil conservation and sediment transport will include the geomorphological map of both basins, as geomorphology reflects the long-term average response of soil erosion processes (López-Vicente et al., 2020). Furthermore, two additional studies are planned: (I) to run AIC together with an erosion model to assess sediment yield at the basin outlet during individual rainfall events (Hao et al., 2022), and (II) to evaluate sediment redistribution throughout the *lameiros*, from the areas bordering the slopes to the areas crossed by watercourses. To carry out the latter task, we will try to obtain/generate a DEM of higher resolution (e.g., 1 × 1 m instead of the current 5 × 5 m), which captures in more detail the topographic parameters associated with the hydrology of *lameiros*.

5. Conclusions

The aggregated index of sediment connectivity (AIC) has demonstrated its ability to calculate in a spatially distributed manner the role that *lameiros* play in the processes of transport and temporary accumulation of sediment, in an environment of headwater hydrological basins with the presence of both permanent and seasonal watercourses. The set of new maps generated and results obtained revealed the different sedimentological scenarios that occur throughout the year: I) at the basin scale, prevalent net export of soil during wet and rainy months (target: watercourses), and temporary accumulation in the watercourses during dry conditions with sediment delivery restricted to the rivers (target: outlet); and II) high connection of *lameiros* with their drainage areas (target: *lameiros*). This study demonstrated that the role played by each input (land-use, soil permeability, rainfall erosivity, slope gradient, drainage area, and roughness of the terrain) heavily relies on the spatial context of each landscape unit concerning the designated target and scenario rather than solely on their values. During dry periods (from May to September), *lameiros* acted as sediment source areas (higher AIC values),–although rainfall erosivity was limited–; and when net soil loss predominated in wet period (from October to April), *lameiros* acted as sedimentation-prone areas (lower AIC values), receiving sediment from slopes (lateral connectivity). Moreover, the connectivity between *lameiros* and their contributing areas exceeded that of other land uses with the outlet and watercourses, effectively acting as sediment disconnectivity areas. The effect of the seasonal changes on functional connectivity differed among scenarios, with minimum changes between the three rainfall erosivity periods (high, moderate and low) when the outlet was the target, and maximum temporal changes when the watercourses were the target due to added effect of the distinct length of the streams during each period. Further research will explore the role of geomorphic elements and sediment redistribution processes within the *lameiros* in greater depth. Besides, we plan to develop a future study focusing on the impact of recurrent wildfires on sediment connectivity in headwater basins, delving deeper into the interactions between land use, fire and functional connectivity. This study highlights the necessity of protecting *lameiros* as a unique and valuable element of the landscape owing to the obtained benefits in terms of sediment dynamics and water regulation.

CRediT authorship contribution statement

T. Bertocco: Writing – original draft, Validation, Software, Methodology, Investigation, Formal analysis, Data curation, Conceptualization. **T. de Figueiredo:** Resources, Investigation, Formal analysis. **A. Paz-González:** Resources, Investigation, Formal analysis. **A. García-Tomillo:** Resources, Investigation, Formal analysis. **M. López-Vicente:** Writing – original draft, Visualization, Validation, Supervision, Software, Resources, Project administration, Methodology, Investigation, Funding acquisition, Formal analysis, Data curation, Conceptualization.

Funding

This research was funded by the project 'Grupo de Referencia Competitiva (GRC) Aquaterra (ED431C 2021/54)' of the Xunta de Galicia. Tamires Bertocco was beneficiary of the grants: "Short Term Scientific Mission (STSM) of the COST Action 'FIRElinks' (E-COST-GRANT-CA18135-2c2072f3)" of the European Commission, and 'Individual research grant 2023.02591.BD' of the Portuguese Foundation for Science and Technology (FCT).

Declaration of competing interest

The authors declare no conflicts of interest.

Acknowledgments

The authors would like to express their sincere gratitude to the reviewers and Editor Dr. Yuichi S. Hayakawa for their valuable feedback and constructive suggestions, which significantly improved the quality of this manuscript.

Appendix A. Supplementary data

Supplementary data associated with this article can be found in the online version at https://doi.org/10.1016/j.geomorph.2025.109750. These data include the Google maps of the most important areas described in this article.

Data availability

Data will be made available on request.

References

Abebe, N., Eekhout, J., Vermeulen, B., Boix-Fayos, C., de Vente, J., Grum, B., Hoitink, T., Baartman, J., 2023. The potential and challenges of the 'RUSLE-IC-SDR' approach to identify sediment dynamics in a Mediterranean catchment. Catena 233, 107480. https://doi.org/10.1016/j.catena.2023.107480.

Agroconsultores and Coba, 1991. Carta dos Solos, Carta do Uso Actual da Terra e Carta da Aptidão da Terra do Nordeste de Portugal. Universidade de Trás-as-Montes e Alto Douro, Vila Real. https://snisolos.dgadr.gov.pt/images/docs/Carta_Solos_Uso_Aptidao_Terra_do_NE_Memorias.pdf (accessed 3.20.2025).

Aguiar, C., Monteiro-Henriques, T., Pires, J., Bastos, P., 2019. Tipologia dos lameiros de Trás-os-Montes. 40ª Reunião de Primavera da SPPF, São Miguel, pp. 48–49. http://hdl.handle.net/10198/21484.Pi (accessed 3.20.2025).

Albert-Belda, E., Bermejo-Fernández, A., Cerdà, A., Taguas, E.V., 2019. The use of Easy-Barriers to control soil and water losses in fire-affected land in Quesada, Andalusia, Spain. Sci. Total Environ. 690, 480–491. https://doi.org/10.1016/j.scitotenv.2019.06.303.

Alder, S., Prasuhn, V., Liniger, H., Herweg, K., Hurni, H., Candinas, A., Gujer, H.U., 2015. A high-resolution map of direct and indirect connectivity of erosion risk areas to surface waters in Switzerland—a risk assessment tool for planning and policy-making. Land Use Policy 48, 236–249. https://doi.org/10.1016/j.landusepol.2015.06.001.

Alvera, B., García-Ruiz, J.M., 2000. Variability of sediment yield from a high mountain catchment, Central Spanish Pyrenees. Arct. Antarct. Alp. Res. 32 (4), 478–484. https://doi.org/10.1080/15230430.2000.12003392.

Asadi, H., Dastorani, M.T., Sidle, R.C., 2023. Estimating index of sediment connectivity using a smart data-driven model. J. Hydrol. 620, 129467. https://doi.org/10.1016/j.jhydrol.2023.129467.

Bakker, M.M., Govers, G., van Doorn, A., Quetier, F., Chouvardas, D., Rounsevell, M., 2008. The response of soil erosion and sediment export to land-use change in four areas of Europe: the importance of landscape pattern. Geomorphology 98 (3–4), 213–226. https://doi.org/10.1016/j.geomorph.2006.12.027.

Barreiro-Lostres, F., Brown, E., Moreno, A., Morellón, M., Abbott, M., Hillman, A., Giralt, S., Valero-Garcés, B., 2015. Sediment delivery and lake dynamics in a Mediterranean mountain watershed: Human-climate interactions during the last millennium (El Tobar Lake record, Iberian Range, Spain). Sci. Total Environ. 533, 506–519. https://doi.org/10.1016/j.scitotenv.2015.06.123.

Bertocco, T., 2021. Caudais de ponta de cheia em bacias de drenagem de lameiros do Parque Natural de Montesinho: estimativas pelo método soil conservation service (SCS) sob cenários de mudança global. Master's final project. Polytechnic Institute of Bragança (IPB), Higher Agrarian School. http://hdl.handle.net/10198/25298.

Bombino, G., Boix-Fayos, C., Cataldo, M.F., D'Agostino, D., Denisi, P., de Vente, J., Labate, A., Zema, D.A., 2020. A modified Catchment Connectivity Index for applications in semi-arid torrents of the Mediterranean environment. River Res. Appl. 36 (5), 735–748. https://doi.org/10.1002/rra.3606.

Borselli, L., Cassi, P., Torri, D., 2008. Prolegomena to sediment and flow connectivity in the landscape: a GIS and field numerical assessment. Catena 75 (3), 268–277. https://doi.org/10.1016/j.catena.2008.07.006.

Buendia, C., Vericat, D., Batalla, R.J., Gibbins, C.N., 2016. Temporal dynamics of sediment transport and transient in-channel storage in a highly erodible catchment. Land Degrad. Dev. 27 (4), 1045–1063. https://doi.org/10.1002/ldr.2348.

Cavalli, M., Trevisani, S., Comiti, F., Marchi, L., 2013. Geomorphometric assessment of spatial sediment connectivity in small Alpine catchments. Geomorphology 188, 31–41. https://doi.org/10.1016/j.geomorph.2012.05.007.

Cerdà, A., Novara, A., Dlapa, P., López-Vicente, M., Úbeda, X., Popović, Z., Mekonnen, M., Terol, E., Janizadeh, S., Mbarki, S., Vogelmann, E.S., Hazrati, S., 2021. Rainfall and water yield in Macizo del Caroig, eastern Iberian Peninsula. Event runoff at plot scale during a rare flash flood at the Barranco de Benacancil. Geogr. Res. Lett. 47 (1), 95–119. https://doi.org/10.18172/cig.4833.

Charraza, A., 2011. Atlas Climático Ibérico/Iberian Climate Atlas. Agencia Estatal de Meteorología, Ministerio de Medio Ambiente y Rural y Marino, Madrid. Instituto de Meteorologia de Portugal. ISBN: 978-84-7837-079-5. https://www.ipma.pt/resources.www/docs_pontuais/ocorrencias/2011/atlas_clima_iberico.pdf.

Colosimo, M.F., Wilcock, P.R., 2007. Alluvial sedimentation and erosion in an urbanizing watershed, Gwynns Falls, Maryland. J. Am. Water Resour. As. 43 (2), 499–521. https://doi.org/10.1111/j.1752-1688.2007.00039.x.

Crema, S., Lanni, C., Goldin, B., Marchi, L., Cavalli, M., 2015. Improvement of a free software tool for the assessment of sediment connectivity. Geoph. Res. Abstracts 17. https://doi.org/10.13140/RG.2.1.2351.2482. EGU2015-7652.

de Figueiredo, T., 2013. Uma panorâmica sobre os recursos pedológicos do Nordeste Transmontano. Escola Superior Agrária, Bragança (Série Estudos; 84). ISBN 978-972-745-138-8. http://hdl.handle.net/10198/8527 (accessed 3.20.2025).

de Santos Loureiro, N., de Azevedo Coutinho, M., 2001. A new procedure to estimate the RUSLE EI30 index, based on monthly rainfall data and applied to the Algarve region. Portugal. J. Hydrol. 250 (1–4), 12–18. https://doi.org/10.1016/S0022-1694(01)00387-0.

DGT – Direção Geral do Território, 2018. Carta de uso e ocupação do solo de Portugal Continental para 2018. Formato Esri Shapefile. Escala 1:25.000. https://snig.dgterritorio.gov.pt/rndg/srv/por/catalog.search#/search?anysnig=COS%202018&fast=index (accessed 3.20.2025).

Diodato, N., 2004. Estimating RUSLE's rainfall factor in the part of Italy with a Mediterranean rainfall regime. Hydrol. Earth Syst. Sci. 8 (1), 103–107. https://doi.org/10.5194/hess-8-103-2004.

Doten, C.O., Bowling, L.C., Lanini, J.S., Maurer, E.P., Lettenmaier, D.P., 2006. A spatially distributed model for the dynamic prediction of sediment erosion and transport in mountainous forested watersheds. Water Resour. Res. 42 (2). https://doi.org/10.1029/2004WR003829.

Duan, T., Li, Y., 2023. A multiscale analysis of the spatially heterogeneous relationships between non-point source pollution–related processes and their main drivers in Chaohu Lake watershed, China. Environ. Sci. Pollut. Res. 30, 86940–86956. https://doi.org/10.1007/s11356-023-28233-1.

EEA – European Environment Agency, 2020. Corine Land Cove (CLC) 2018. version 2020_20u1. https://land.copernicus.eu/en/products/corine-land-cover/clc2018 (accessed 3.20.2025).

Fernandes, F., 2019. Efeito do abandono em propriedades físico-químicas do solo em lameiros do Parque Natural de Montesinho. Master's final project. Polytechnic Institute of Bragança (IPB), Higher Agrarian School. http://hdl.handle.net/10198/22752.

Fogaça-Neto, J.A., 2022. Caracterização das bacias de drenagem dos lameiros da Alta Lombada e Onor, Parque Natural de Montesinho [Doctoral dissertation]. Polytechnic Institute of Bragança, Portugal. http://hdl.handle.net/10198/25389.

Food and Agriculture Organization of the United Nations (FAO), 1981. FAO soils portal. https://www.fao.org/soils-portal/soil-survey/soil-%20maps-and-databases/faounesco-soil-map-of-the-world/en/ (accessed 6.20.2023).

Fortesa, J., Latron, J., García-Comendador, J., Company, J., Estrany, J., 2020. Runoff and soil moisture as driving factors in suspended sediment transport of a small mid-mountain Mediterranean catchment. Geomorphology 368, 107349. https://doi.org/10.1016/j.geomorph.2020.107349.

Galia, T., Škarpich, V., Ruman, S., 2021. Impact of check dam series on coarse sediment connectivity. Geomorphology 377, 107595. https://doi.org/10.1016/j.geomorph.2021.107595.

González-Romero, J., López-Vicente, M., Gómez-Sánchez, E., Peña-Molina, E., Galletero, P., Plaza-Alvarez, P., Moya, D., De las Heras, J., Lucas-Borja, M.E., 2021. Post-fire management effects on sediment (dis)connectivity in Mediterranean forest ecosystems: Channel and catchment response. Earth Surf. Proc. Land. 46, 2710–2727. https://doi.org/10.1002/esp.5202.

González-Romero, J., López-Vicente, M., Gómez-Sánchez, E., Peña-Molina, E., Galletero, P., Plaza-Alvarez, P., Fajardo-Cantos, A., Moya, D., De las Heras, J., Lucas-Borja, M.E., 2022. Post-fire management effects on hillslope-stream sediment connectivity in a Mediterranean forest ecosystem. J. Environ. Manage. 316, 115212. https://doi.org/10.1016/j.jenvman.2022.115212.

Hao, R., Huang, X., Cai, Z.W., Xiao, H.B., Wang, J., Shi, Z.H., 2022. Incorporating sediment connectivity index into MUSLE model to explore soil erosion and sediment yield relationships at event scale. J. Hydrol. 614, 128579. https://doi.org/10.1016/j.jhydrol.2022.128579.

Hooke, J., Souza, J., Marchamalo, M., 2021. Evaluation of connectivity indices applied to a Mediterranean agricultural catchment. Catena 207, 105713. https://doi.org/10.1016/j.catena.2021.105713.

Kasai, M., Brierley, G.J., Page, M.J., Marutani, T., Trustrum, N.A., 2005. Impacts of land use change on patterns of sediment flux in Weraamaia catchment, New Zealand. Catena 64 (1), 27–60. https://doi.org/10.1016/j.catena.2005.06.014.

Kosztra, B., Büttner, G., Hazeu, G., Arnold, S., 2019. Updated CLC illustrated nomenclature guidelines. In: European Topic Centre on Urban, Land and Soil Systems (ETC/ULS). European Environment Agency, Wien, Austria, pp. 1–124. https://land.copernicus.eu/content/corine-land-cover-nomenclature-guidelines/docs/pdf/CLC2018_Nomenclature_illustrated_guide_20190510.pdf.

Liu, W., Shi, C., Ma, Y., Wang, Y., 2022. Evaluating sediment connectivity and its effects on sediment reduction in a catchment on the Loess Plateau, China. Geoderma 408, 115566. https://doi.org/10.1016/j.geoderma.2021.115566.

Llena, M., Batalla, R.J., Smith, M.W., Vericat, D., 2021. Do badlands (always) control sediment yield? Evidence from a small intermittent catchment. Catena 198, 105015. https://doi.org/10.1016/j.catena.2020.105015.

López-Vicente, M., Ben-Salem, N., 2019. Computing structural and functional flow and sediment connectivity with a new aggregated index: a case study in a large Mediterranean catchment. Sci. Total Environ. 651, 179–191. https://doi.org/10.1016/j.scitotenv.2018.09.170.

López-Vicente, M., Lana-Renault, N., García-Ruiz, J.M., Navas, A., 2011. Assessing the potential effect of different land cover management practices on sediment yield from an abandoned farmland catchment in the Spanish Pyrenees. J. Soil. Sediment. 11, 1440–1455. https://doi.org/10.1007/s11368-011-0428-2.

López-Vicente, M., Quijano, L., Gaspar, L., Palazón, L., Navas, A., 2015. Severe soil erosion during a 3-day exceptional rainfall event: combining modelling and field data for a fallow cereal field. Hydrol. Process. 29 (10), 2358–2372. https://doi.org/10.1002/hyp.10370.

López-Vicente, M., Sun, X., Onda, Y., Kato, H., Gomi, T., Hiraoka, M., 2017. Effect of tree thinning and skidding trails on hydrological connectivity in two Japanese forest catchments. Geomorphology 292, 104–114. https://doi.org/10.1016/j.geomorph.2017.05.006.

López-Vicente, M., González-Romero, J., Lucas-Borja, M.E., 2020. Forest fire effects on sediment connectivity in headwater sub-catchments: evaluation of indices performance. Sci. Total Environ. 732, 139206. https://doi.org/10.1016/j.scitotenv.2020.139206.

López-Vicente, M., Kramer, H., Keesstra, S., 2021. Effectiveness of soil erosion barriers to reduce sediment connectivity at small basin scale in a fire-affected forest. J. Environ. Manage. 278, 111510. https://doi.org/10.1016/j.jenvman.2020.111510.

Mangi, H.O., Onywere, S.M., Kitur, E.C., Lalika, M.C., Chilagane, N.A., 2022. Hydrological response to land use and land cover change on the slopes of Kilimanjaro and Meru Mountains. Ecohydrology & Hydrobiology 22 (4), 609–626. https://doi.org/10.1016/j.ecohyd.2022.08.002.

Marques, S.M., Campos, F.S., David, J., Cabral, P., 2021. Modelling sediment retention services and soil erosion changes in Portugal: a spatio-temporal approach. ISPRS Int. J. Geo-Information 10 (4), 262. https://doi.org/10.3390/ijgi10040262.

Martini, L., Cavalli, M., Picco, L., 2022. Predicting sediment connectivity in a mountain basin: a quantitative analysis of the index of connectivity. Earth Surf. Proc. Land. 47 (6), 1500–1513. https://doi.org/10.1002/esp.5331.

Nadal-Romero, E., Lasanta, T., García-Ruiz, J.M., 2013. Runoff and sediment yield from land under various uses in a Mediterranean mountain area: long-term results from an experimental station. Earth Surf. Proc. Land. 38 (4), 346–355. https://doi.org/10.1002/esp.3281.

Najafi, S., Sadeghi, S.H., Heckmann, T., 2021. Analysis of sediment accessibility and availability concepts based on sediment connectivity throughout a watershed. Land Degrad. Dev. 32 (10), 3023–3044. https://doi.org/10.1002/ldr.3964.

Nosrati, K., Collins, A.L., 2019. Investigating the importance of recreational roads as a sediment source in a mountainous catchment using a fingerprinting procedure with different multivariate statistical techniques and a Bayesian un-mixing model. J. Hydrol. 569, 506–518. https://www-sciencedirect-com.accedys.udc.es/science/article/pii/S0022169418309685.

Panagos, P., Borrelli, P., Meusburger, K., Alewell, C., Lugato, E., Montanarella, L., 2015. Estimating the soil erosion cover-management factor at the European scale. Land Use Policy 48, 38–50. https://doi.org/10.1016/j.landusepol.2015.05.021.

Parsons, A.J., Wainwright, J., Brazier, R.E., Powell, D.M., 2006. Is sediment delivery a fallacy? Earth Surf. Proc. Land. 31 (10), 1325–1328. https://doi.org/10.1002/esp.1395.

Pereira, E., Arrobas, M., 2010. Caracterização da fertilidade química de lameiros do nordeste transmontano. In: IV Reunião Ibérica de Pastagens e Forragens, pp. 81–86. Zamora. http://hdl.handle.net/10198/3904.

Pereira, L.S., Sousa, V.S., 2005. Lameiros e prados de lima, uma paisagem das terras altas húmidas de Portugal. V Seminário Internacional CYTED-XVII. Un enfoque para la gestión sustentable del agua: Experiencias en zonas húmedas. Universidad de Buenos Aires, Buenos Aires, Argentina, p. 12.

Pereira, P., Pereira, D.I., Alves, M.I.C., Meireles, C., 2003. Geomorfologia do Parque Natural de Montesinho: controlo estrutural e superfícies de aplanamento. In: VI Congresso Nacional de Geologia, Monte de Caparica, 4 a 6 de Junho de 2003: [Comunicações], 2003. Universidade Nova de Lisboa, Faculdade de Ciências e Tecnologia, Monte de Caparica, pp. C61–C64. CD-ROM. http://hdl.handle.net/10400.9/974.

Pires, J., Pinto, P.A., Moreira, N., 1994. Lameiros de Trás-os-Montes: perspectivas de futuro para estas pastagens de montanha. Instituto Politécnico de Bragança, Escola Superior Agrária – ESA, p. 29. Série Estudos. ISBN 972-745-025-3. http://hdl.handle.net/10198/7717.

PNOA, 2020. Ministerio de Transportes, Movilidad y Agenda Urbana. Instituto Geográfico Nacional (2023). Plan Nacional de Ortofotografía Aerea. https://centrodedescargas.cnig.es/CentroDescargas/busquedaSerie.do?codSerie=POA10.

Poças, I., Cunha, M., Pereira, L.S., 2006. Pastagens seminaturais de montanha: Lameiros, sistemas ancestrais no século XXI. Taller CYTED XVII, El agua en Ibero-América: Tecnologías apropiadas y tecnologías ancestrales. Universidad Nacional de Piura-Perú, Lima. https://www.fc.up.pt/LamSat_XXI/artigos/Taller2009.pdf.

Poças, I., Pereira, L.S., Cunha, M., 2007. Pastagens como factor de conservação da água em zonas de montanha, os lameiros. Pastagens e Forragens 28, 59–77. https://www.fc.up.pt/LamSat_XXI/artigos/Pastagens&Forragens.pdf.

Poças, I., Cunha, M., Marçal, A.R.S., Pereira, L.S., 2009. Los Lameiros, pastizales seminaturales de regadio de montaña: sistemas ancestrales en el paisaje rural portugués del siglo XXI. In: Saldaña Martinez, T., Palerme, J., Castro, M., Pereira, L. S. (Eds.), Riegos Ancestrales de Iberoamerıca. Técnicas y Organización Social del Pequeño Riego. Colegio de Postgraduados e Mundi Prensa México, México D.F, pp. 27–40.

Poças, I., Cunha, M., Pereira, L.S., 2012. Dynamics of mountain semi-natural grassland meadows inferred from SPOT-VEGETATION and field spectroradiometer data. Int. J. Remote Sens. 33 (14), 4334–4355. https://doi.org/10.1080/01431161.2011.645084.

Poças, I., Cunha, M., Pereira, L.S., Allen, R.G., 2013. Using remote sensing energy balance and evapotranspiration to characterize montane landscape vegetation with focus on grass and pasture lands. Int. J. Appl. Earth Obs. 21, 159–172. https://doi.org/10.1016/j.jag.2012.08.017.

Ranzan, A.P., 2020. Caracterização das bacias de drenagem dos lameiros da Alta Lombada e Onor, Parque Natural de Montesinho [Doctoral dissertation]. Polytechnic Institute of Bragança. http://hdl.handle.net/10198/23185.

Ribeiro, S., Monteiro, A., 2014. Permanent pastures in mountain areas: characterization, management and conservation. Revista de Ciências Agrárias (Portugal) 37 (2), 131–140. https://www.cabidigitallibrary.org/doi/pdf/10.5555/20143319089.

Rodrigues, A., Santiago, A., Laím, L., Viegas, D.X., Zêzere, J.L., 2022. Rural fires—causes of human losses in the 2017 fires in Portugal. Appl. Sci. 12 (24), 12561. https://doi.org/10.3390/app122412561.

Royer, A.C., de Figueiredo, T., García-Tomillo, A., Dafonte, J., Fonseca, F., Paz González, A., 2020. Tomografía eléctrica resistiva en zonas de montaña: la dinámica del agua en lameiros en el Parque Natural de Montesinho, Portugal. In: X Congreso sobre Uso y Manejo del Suelo Gestión Sostenible de Suelos y Recursos Hídricos. Universidade da Coruña, p. 57. http://hdl.handle.net/10198/25128.

Souza, J., Hooke, J., 2021. Influence of seasonal vegetation dynamics on hydrological connectivity in tropical drylands. Hydrol. Proc. 35 (11), e14427. https://doi.org/10.1002/hyp.14427.

Stavi, I., Siad, S.M., Kyriazopoulos, A.P., Halbac-Cotoara-Zamfir, R., 2020. Water runoff harvesting systems for restoration of degraded rangelands: a review of challenges and opportunities. J. Environ. Manage. 255, 109823. https://doi.org/10.1016/j.jenvman.2019.109823.

Swarnkar, S., Sinha, R., Tripathi, S., 2020. Morphometric diversity of supply-limited and transport-limited river systems in the Himalayan foreland. Geomorphology 348, 106882. https://doi.org/10.1016/j.geomorph.2019.106882.

Tang, B., Jiao, J., Zhang, Y., Chen, Y., Wang, N., Bai, L., 2020. The magnitude of soil erosion on hillslopes with different land use patterns under an extreme rainstorm on the Northern Loess Plateau, China. Soil Till. Res. 204, 104716. https://doi.org/10.1016/j.still.2020.104716.

Teles, A.N., 1970. Os lameiros de montanha do norte de Portugal. Subsídios para a sua caracterização fitossociológica e química. In: Separata da Agronomia Lusitana – Vol. XXXI – Tomo I – II. 141 p. https://catalogo.biblioteca.utad.pt/cgi-bin/koha/opac-detail.pl?biblionumber=56589.

Terêncio, D.P.S., Vitor Cortes, R.M., Leal Pacheco, F.A., Moura, J.P., Sanches Fernandes, L.F., 2020. A method for estimating the risk of dam reservoir silting in fire-prone watersheds: a study in Douro River, Portugal. Water 12 (11), 2959. https://doi.org/10.3390/w12112959.

Tola, S.Y., Shetty, A., 2021. Land cover change and its implication to hydrological regimes and soil erosion in Awash River basin, Ethiopia: a systematic review. Environ. Monit. Assess. 193 (12), 1–19. https://doi.org/10.1007/s10661-021-09599-6.

Torresani, L., Piton, G., D'Agostino, V., 2023. Morphodynamics and sediment connectivity index in an unmanaged, debris-flow prone catchment: a through time perspective. J. Mt. Sci. 20 (4), 891–910. https://doi.org/10.1007/s11629-022-7746-2.

van den Dries, A., 2002. The Art of Irrigation. The Development, Stagnation and Redesign of Farmer-Managed Irrigation Systems in Northern Portugal. Proefschrift. ter verkrijging van de rector magnificus van Wageningen Universiteit, p. 36.

van der Grift, S., 2021. The Effect of Wildfires on Sediment Connectivity Using the AIC Method. Long Term Analysis for the Águeda Catchment in Portugal From 1979 Until 2019. MSc thesis.. Wageningen University & Research, Wageningen, The Netherlands.

Vieira, J., Gonçalves, S., Sanches, D., Bernardo, A., Moreira, N., 2000. Sustentabilidade dos lameiros e do sistema de agricultura de montanha do Norte de Portugal. II. Lameiros. In: 3 Reunião Ibérica de Pastagens e Forragens. Consellería de Agricultura, Ganadería e Política Agroalimentaria, pp. 737–742.

Vieira, D.C.S., Malvar, M.C., Martins, M.A.S., Serpa, D., Keizer, J.J., 2018. Key factors controlling the post-fire hydrological and erosive response at micro-plot scale in a recently burned Mediterranean forest. Geomorphology 319, 161–173. https://doi.org/10.1016/j.geomorph.2018.07.014.

Wang, S., Yao, A., Zhao, X., 2014. Analyzing hydrological connectivity for a slope-surface on the basis of rainfall simulation experiment. Adv. Water Sci. 25 (4), 526–533. http://skxjz.nhri.cn/en/article/id/2435.

Wu, J., Baartman, J.E.M., Nunes, J.P., 2021. Comparing the impacts of wildfire and meteorological variability on hydrological and erosion responses in a Mediterranean catchment. Land Degrad. Dev. 32 (2), 640–653. https://doi.org/10.1002/ldr.3732.

Wu, Z., Baartman, J.E.M., Nunes, P.J., López-Vicente, M., 2023. Intra-annual sediment dynamic assessment in the Wei River Basin, China, using the AIC functional-structural connectivity index. Ecol. Indic. 146, 109775. https://doi.org/10.1016/j.ecolind.2022.109775.

Xu, G., Cheng, Y., Zhao, C., Mao, J., Li, Z., Jia, L., Zhang, Y., Wang, B., 2023. Effects of driving factors at multi-spatial scales on seasonal runoff and sediment changes. Catena 222, 106867. https://doi.org/10.1016/j.catena.2022.106867.

Yan, X.-Q., Jiao, J.-Y., Tang, B.-Z., Liang, Y., Wang, Z.-J., 2022. Assessing sediment connectivity and its spatial response on land use using two flow direction algorithms in the catchment on the Chinese Loess Plateau. J. Mt. Sci. 19 (4), 1119–1138. https://doi.org/10.1007/s11629-021-6936-7.

Zanandrea, F., Michel, G.P., Kobiyama, M., Censi, G., Abatti, B.H., 2021. Spatial-temporal assessment of water and sediment connectivity through a modified connectivity index in a subtropical mountainous catchment. Catena 204, 105380. https://doi.org/10.1016/j.catena.2021.105380.